ALESSANDRA TESTA, KONSTANTIN BOSS[1]

WHAT GOES AROUND COMES AROUND: THE US CLIMATE-ECONOMIC CYCLE

Abstract. We use a spatial data set of US temperatures in a factor-augmented VAR to quantify the contribution of the US economy to fluctuations in temperatures over the past 70 years. We show that there are at least five distinct sources of broad scale temperature fluctuations in the US and uncover a strong relationship of temperatures with aggregate productivity. Disentangling natural from anthropogenic effects, we find that economic expansions do not only lead to warming: technology improvements initially decrease temperatures, whereas investment and labor supply shocks increase them rapidly and persistently. This happens because the cooling effect of aerosol emissions initially outweighs the warming effect from greenhouse gases for technology shocks, but not for investment and labor supply shocks. Taken together, these economic shocks explain around 25% of long-term temperature variation in the US. In turn, temperature shocks induce small contractions in aggregate GDP, but can even be beneficial for the economy, when they predominantly hit the western states.

Keywords. Factor-augmented VAR, climate econometrics, temperature shocks, frequency domain identification

1. INTRODUCTION

The rise in global socio-economic activity and the accompanying increase in anthropogenic greenhouse gas (GHG) emissions that characterized the past century are known to be important causes of global warming. Worldwide average surface temperatures have already increased by 1.1°C since the industrial revolution and are projected to increase by between 1.4°C and 4.4°C until 2100 (IPCC, 2023). In turn, temperature increases can lead to lower agricultural yields (Deschênes and Greenstone, 2007), more premature deaths (Barreca *et al.*,

[1] Boss acknowledges funding under the FPI Grant PRE2020-093941 funded by MCIN/AEI/10.13039/501100011033 and by ESF Investing in your future. We would like to thank Selim Elbadri for a very helpful discussion. We also thank Luca Gambetti, Sarah Zoi, Marco Mazzali, Luca Sala, Tajana Dahlhaus and Christian Brownlees as well as seminar participants at the 64th Annual Conference of the Italian Economic Association (Società Italiana di Economia -SIE), the Banco de España, the Ruhr Graduate School Doctoral Conference, Dynamic Econometrics at Oxford, the JRC Ispra, the Centro Einaudi Torino as well as of the Bellaterra Macro Club for their very valuable comments. We are also grateful to the Centro Einaudi Torino for awarding one of the Giorgio Rota Best Paper Awards 2024 to this paper.

2015), and diminished productivity (Burke *et al.*, 2015), resulting in potentially severe losses in welfare (Bilal and Känzig, 2024).

In this paper, we develop an empirical framework for the United States (US) to study how economic activity has affected temperatures and vice versa. We use a factor-augmented vector autoregression (FAVAR; Bernanke *et al.*, 2005) to model the dynamics of US temperatures on a $0.5° \times 0.5°$ spatial grid together with key macroeconomic aggregates. To disentangle the effect of human activity on temperatures from the effect of temperatures on human activity, we rely on the notion of structural shocks that is common in causal macroeconomic inference (Ramey, 2016). We use partial identification techniques to pin down three well-established economic shocks in the frequency domain along the lines of Forni *et al.* (2023). First, a technology shock is identified as the main contributor to low-frequency variation in utilization-adjusted TFP, similar to DiCecio and Owyang (2010) and Dieppe *et al.* (2021). Second, conditional on the technology shock, we identify an investment shock in the spirit of Justiniano et al. (2010, 2011) and Auclert *et al.* (2020) as the main driver of business-cycle fluctuations in investment. Third, similar to Shapiro and Watson (1988), we identify a labor supply shock as the main driver of the low-frequency component of hours worked, conditional on both the technology and investment shocks. On the other hand, we rely on statistical arguments to identify temperature shocks. As Angeletos *et al.* (2020) identify an economic "main business-cycle shock," we apply a similar reasoning to capture the main drivers of temperature fluctuations in specific geographic areas, such as the west coast, the east coast, the Gulf region, or the non-coastal states, as well as in specific frequency bands, for example, at the El Niño-La Niña periodicities. We then compute the impulse responses of US real GDP to these shocks.

Based on our analysis, we report the following qualitative results: First, it is insufficient to rely on a single measure of national temperatures such as (weighted) averages, as is frequently done in the literature (Dell *et al.*, 2012; Burke *et al.*, 2015; Acevedo *et al.*, 2020). This is because there is a lower bound of five large shocks driving US temperatures. Average temperatures alone only reflect variation in the Midwest region and neglect temperature changes in the economically important coastal areas. This happens because the American Midwest is affected by strong cold air flows from the North and warm air flows from the South, leading to very high temperature variability (Kunkel *et al.*, 2013). Geographic heterogeneity also matters for the effect of temperatures on aggregate GDP, a crucial relationship for environmental policy-making: If warming affects only the west of the country, this can be net positive for the economy, whereas temperature increases generally diminish output slightly. Second, we provide evidence for a relationship between temperatures and socio-economic activity mostly through changes in TFP. A loss in productivity is thought to be one of the main channels for the negative effects of temperature warming (Burke et al., 2015). We argue along the lines of Pretis (2021) that it is important to properly distinguish if temperature fluctuations cause productivity changes or vice versa. In the case of the US, we find that the majority of the negative co-movement between temperatures and TFP is caused by economic shocks.

In addition, we contribute the following quantitative findings to the literature: First, on average, a quarter of the low-frequency component of US temperatures can be attributed to the three economic shocks, with technology shocks accounting for 10%, investment shocks for 11%, and labor supply shocks for 4%. In the east and south of the US, where manufacturing and natural resource processing are concentrated, the explained variation from technology shocks alone can be as high as 35%. High and medium cycle variations of temperatures, on the other hand, are not strongly explained by anthropogenic shocks. The economic shocks have small, yet persistent effects on temperatures. While technology shocks initially decrease temperatures in the industrial part of the country, this effect recedes in the long run despite the permanent effect on economic activity and emissions. Investment shocks and labor supply shocks lead to geographically homogeneous warming, in the area of 0.01°C, even though the economic expansion is mostly transitory. We argue that decreases in temperatures can be explained by a stronger effect of aerosol emissions than GHG emissions, whereas warming is observed when aerosols are removed and GHGs emitted. Second, central US and east coast-centered increases of 1°C lead to mild losses of aggregate GDP around 0.1%–0.13%. This is in line with the view that the US, for the most part, has been close to a bliss point where temperature warming has so far had essentially zero aggregate effects (see, e.g., Dell *et al.*, 2012; Nath *et al.*, 2023; Natoli, 2023). However, shocks that predominantly affect temperatures on the west coast can have expansionary effects. We find them to lead to up to 0.29% higher GDP after an initial decrease of around 0.32%. This is because when increases in temperatures occur in the west, they are accompanied by decreases in the east. The net effect of this is positive for aggregate real GDP. Temperature shocks are not persistent for temperatures anywhere in the US.

Comprehensive overviews of the climate-econometric literature are provided by Newell et al. (2021) and de Juan *et al.* (2022). The authors show that especially the estimates of economic damages from climate change vary substantially across methodologies. We relate to and expand the literature that quantifies the effect of temperatures on the US economy. Important contributions over the existing empirical literature are as follows: We identify the direct effect on temperatures of economic shocks that explain the bulk of macroeconomic fluctuations. This is necessary because policy-oriented models such as Cai and Lontzek (2019) focus on damages from temperature changes induced by such economic shocks on the economy, although usually relying on TFP shocks alone. In addition, we allow the data to determine the timing of the effects of emissions on temperatures rather than assuming that economic activity translates into temperature changes with a delay of a year, as is customary in the literature (e.g., Donadelli *et al.*, 2017; Goulet Coulombe and Göbel, 2021), since this is not supported by climate research (e.g., Joos *et al.*, 2013; Forster *et al.*, 2020). Instead, we propose an identification based on statistical arguments with no implied timing restrictions.

Other studies in this area use mostly panel regressions without dynamic causal response estimates (e.g., Deryugina and Hsiang, 2014; Colacito *et al.*, 2019; Gourio and Fries, 2020), which are less focused on the transmission mechanism of temperature fluctuations to the real economy. Kaufmann *et al.* (2013), Montamat and Stock (2020), and Stock (2020) discuss economic processes affecting climate forcing (and thus temperatures), but do not identify the stochastic processes explicitly. Empirical studies that compute the effects of economic shocks on US CO_2 emissions are Khan *et al.* (2019), Fosten (2019), and Bennedsen *et al.* (2021), however, no explicit connection to temperature changes is made. Since the effect of economic activity on temperatures is not exclusively driven by GHG emissions, but also other gases such as aerosols, Magnus et al. (2011), Storelvmo *et al.* (2016), Phillips *et al.* (2020) provide a breakdown of the respective warming and cooling effects. We show that the aerosol cooling effect prevails for technology shocks, whereas other business cycle shocks lead to warming through a dominant impulse of GHGs. From a methodological view, our paper is closely related to Mumtaz and Marotta (2023), Berg *et al.* (2023), and Bastien-Olvera *et al.* (2022). The first two for the authors' use of a factor structure for temperature dynamics and the third one for the frequency domain decomposition of temperatures. While Mumtaz and Marotta (2023) use global data to characterize patterns of aggregate temperature movements, their study focuses on correlations with economic development indicators. We provide causal interpretations for the variations in temperature data and vice versa. Berg *et al.* (2023) consider only a single factor for their global data set, whereas we show that this captures a very localized temperature phenomenon. Bastien-Olvera *et al.* (2022) regress GDP growth onto the low-frequency component of average temperatures extracted using a low-pass filter. However, as we show, this component is substantially affected by economic shocks, for which the authors do not control.

The rest of the paper is organized as follows: Section 2 describes the temperature and economic data we use in the empirical model, Section 3 introduces the model and explains the identification methodology, Section 4 presents the findings, which are discussed in Section 5. Finally, Section 6 concludes.

2. Data

Temperature data are obtained from the Terrestrial Air Temperature and Precipitation 1900–2017 Gridded Monthly dataset (Matsuura and Willmott, 2018), which provides monthly mean temperatures over land at a 0.5 × 0.5 degree resolution for the entire globe. The authors compute the monthly average gridded data from daily weather station records, considering only stations for which no more than five daily data points in a given month are missing. The grid cell data are estimated from measurement station averages through spatial interpolation. Outliers and unrealistic values that might arise due to measurement error are removed by the authors.

3,325 of the grid points are located in the contiguous United States (i.e., excluding Alaska, Hawaii, and the US territories). We aggregate the monthly data to a quarterly frequency by taking the average over the three months in a quarter and seasonally adjust each time series using the deseason() function of the MATLAB Climate Data Toolbox (Greene *et al.*, 2019), which centers and linearly detrends each time series and then removes the climatology, i.e., the average of each given month in a year. In addition, we weight each grid point by the square root of the cosine of the latitude in the center of the cell. This is common practice in the literature that computes empirical orthogonal functions (EOFs) from climate data (Hannachi *et al.*, 2007) and serves as a means to account for the arc of the earth, which changes the size of degree-based grid cells further away from the equator relative to those that are closer to the equator. EOFs are, in essence, the loadings of the principal components computed for gridded climate data, which can be used to detect patterns such as the El Niño Southern Oscillation (ENSO) (Erichson *et al.*, 2020).

We use this method to summarize the information contained in the gridded land surface temperature dataset. To determine the number of principal components, we use the criterion of Alessi et al. (2010), which suggests using between 8 and 17 factors. For parsimony, we set the number of principal components to r=8r=8 and study the effect of choosing r=17r=17 in a robustness exercise. Figure 1 shows that the time series for average US temperature and the first principal component from our dataset are 96% correlated. In addition, Figure 2 shows that the first principal component – which carries the same signal as the average –explains temperature variation only in the Midwest of the US, while important economic centers such as the coastal areas are much less well explained. Expanding the information to r=8r=8 yields much higher explained variation, in the area of 80% almost everywhere in the US. Similar results appear in other large countries of the world, but are not reported here. Therefore, the information in average temperatures covered by a single principal component is clearly insufficient to capture the full temperature dynamics of the US. Any approach using only nationwide averages will likely miss important spatial temperature information.

FIGURE 1 • AVERAGE TEMPERATURES IN THE US AND FIRST PRINCIPAL COMPONENT. Correlation is 96%

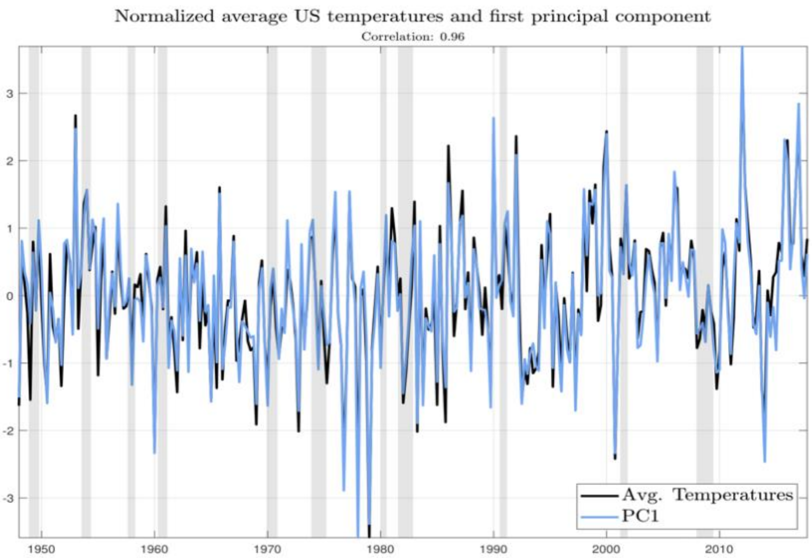

FIGURE 2 • R^2 FROM REGRESSION OF GRID CELL TEMPERATURES ON PRINCIPAL COMPONENTS

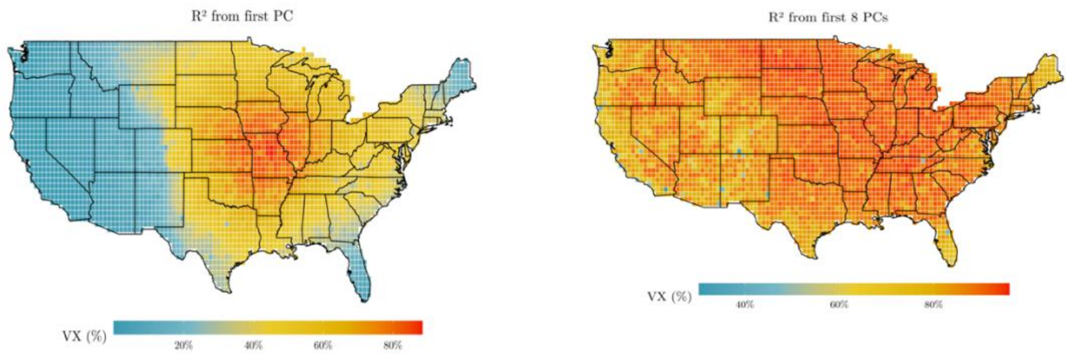

a) First PC

b) First 8 PCs

The economic data we include are real GDP, real investment, nonfarm-business sector hours worked (obtained from FRED), and utilization-adjusted TFP (from Fernald, 2014). All economic variables enter the model in log-levels to account for the possibility of co-integration among economic and climate variables, as pointed out in Pretis (2020). We have checked the model in per-capita terms and found no major difference. A detailed account of all the economic data used in this paper and their construction is given in the Appendix. The sample we use for estimation of the baseline model runs at quarterly frequency from 1948 to 2017.

Figure 3 plots the economic data together with the trend in average US temperatures. Temperatures exhibit an initial decrease until around the 1970s, after which they trend upwards. The series appear to share a common trend as of the 1970s but diverge again after the Great Recession, where the growth rate in temperatures speeds up.

FIGURE 3 • HP-FILTERED TREND IN MEAN CONTIGUOUS US TEMPERATURES ($\lambda = 160000$) AND LOGARITHMIZED ECONOMIC TIME SERIES
Shaded areas are NBER recessions. All data are centered and scaled To have zero mean and unit variance

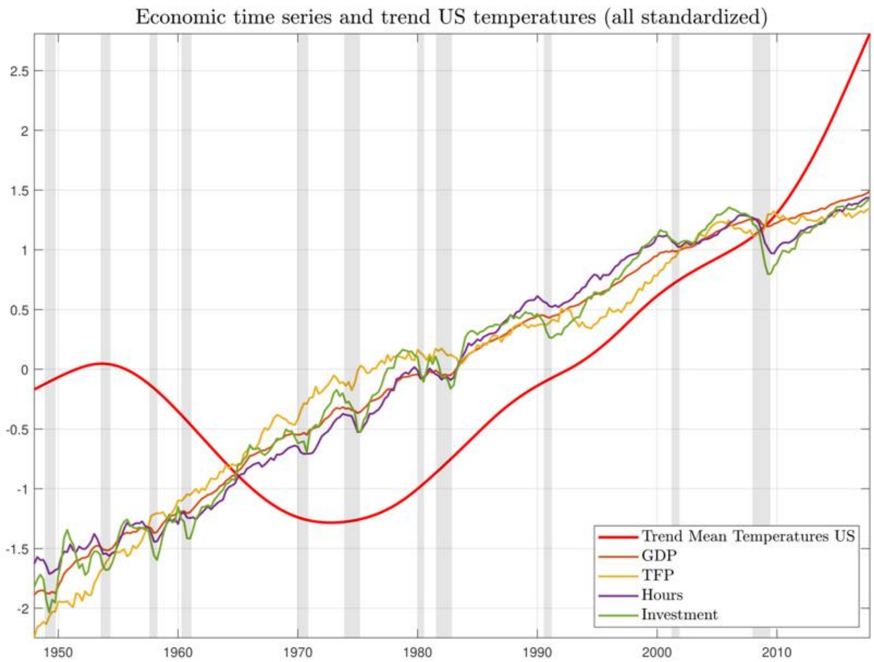

3. ECONOMETRIC METHODOLOGY

3.1. Reduced form data representation

Our estimation procedure is carried out in two steps, as in factor-augmented vector autoregressions (FAVAR) (e.g., Bernanke *et al.* (2005)) and dynamic factor models (DFM) (e.g., Forni *et al.* (2009)). These models have the advantage that they can accommodate datasets with many time series and allow for the straightforward identification of structural shocks and their propagation through the methods common in the literature on structural VARs (SVARs) (Ramey, 2016).

The model for the temperatures at grid cell i at time t is given by:

$$T_{it} = \lambda_i Y_t + \eta_{it} \quad (1)$$

where T_{it} are the raw temperatures and η_{it} is the idiosyncratic component. The vector of loadings λ_i captures the sensitivity of temperatures at grid cell i to the aggregate variables in the vector $Y_t = [f_t, y_t]'$. We combine the principal components f_t of the temperature data with the selected set of economic variables Y_t. This is a simple version of the model in Phillips et al. (2020), where we accommodate spatial dependence of temperatures on common factors. The reduced form model for Y_t is a VAR of lag order p:

$$A(L)Y_t = \mu + \epsilon_t, \quad \epsilon_t \sim WN(0, \Sigma) \tag{2}$$

where μ is a constant term, $A(L)$ is a matrix polynomial in the lag operator given by $A(L) = A_0 + A_1L + A_2L^2 + \cdots + A_pL^p$, and ϵ_t is a vector of reduced form white noise errors whose variance-covariance matrix is given by Σ. Treating the principal components f_t as observed, model (2) is efficiently estimated using OLS for each equation. The lag order is determined using the Akaike information criterion, which yields $p = 2$. Higher lag orders do not change our results substantially. The reduced form VAR in (2) is assumed to admit a moving average (MA) representation given by:

$$Y_t = C(L)\epsilon_t \tag{3}$$

where $C(L)$ is obtained by inverting $A(L)$, and we have dropped the constant as it is immaterial for our identification strategy and the model dynamics.

3.2. Identification

To identify economic and temperature shocks, we rely on techniques that have been proposed for the study of business cycle fluctuations. Most environmental models focus on aggregate productivity shocks as drivers of emissions (Annicchiarico and Di Dio, 2021). However, the recent contributions by Angeletos *et al.* (2020) and Forni *et al.* (2023) have shown that the economy, and by extension also emissions, fluctuates largely because of sources that are not purely related to movements in TFP. Therefore, our analysis is set up to provide evidence on alternative channels for the effect of socio-economic activity on temperatures, beyond RBC-style technology shocks alone. It is most common to distinguish fluctuations of high frequency, business cycle frequency, and low frequency. Table (1) shows the definitions of frequency bands we adopt for our purposes:

TABLE 1 • FREQUENCY BANDS ADOPTED FOR IDENTIFICATION

Frequency	Low	Business Cycle	High	Full Spectrum
Quarters	> 40	$[6, 32]$	$(0, 6]$	$(0, \infty)$

The business cycle frequency is between 6 (1.5 years) and 32 quarters (8 years), as is common in the economic literature (Angeletos *et al.*, 2020). This definition roughly coincides with medium cycles that are observable in climatic data as well. For example, ENSO (El Niño-Southern Oscillation) influences global weather and occurs every 3-5 years and lasts for roughly a year (NOAA, 2023). The higher frequencies coincide with the strongest fluctuations in our temperature data. This component is most similar to the types of weather shocks usually identified in the literature. The low-frequency band is where we expect the strongest influence of socio-economic activity to show up, as it contains the slight upward trend in the data that is believed to be caused by human beings. Allowing the medium-cycle band to include a few more years (e.g., to include the 11-year solar cycles) does not affect our results.

The structural MA representation of (3) is given by

$$\boldsymbol{Y_t = C(L)SHu_t = D(L)Hu_t = K(L)u_t, \quad u_t \sim WN(0, I)} \tag{4}$$

where $\boldsymbol{SS'} = \boldsymbol{\Sigma}, \boldsymbol{HH'} = \boldsymbol{I}$, and $\boldsymbol{u_t} = \boldsymbol{H'S^{-1}\epsilon_t}$. Identification of the structural shocks boils down to pinning down columns of the orthonormal matrix $\boldsymbol{H}$. The impulse responses of the economic variables (subindex E) and of temperatures (subindex T) are then given by

$$\boldsymbol{IRF_E = D_E(L)H} \tag{5}$$
$$\boldsymbol{IRF_T = \Lambda D(L)H} \tag{6}$$

The notation $\boldsymbol{D_E(L)}$ is shorthand for selecting the rows from each of the matrices in D$(\boldsymbol{L})$ which correspond to the entries of $\boldsymbol{Y_t}$ that belong to economic variables. $\boldsymbol{\Lambda}$ is the matrix containing the vectors of loadings $\boldsymbol{\lambda_i}$ for each grid cell.

3.2.1. Identification of economic shocks

We identify three economic shocks – a technology shock, an investment shock, and a labor supply shock. These are the three shocks proposed as the main business cycle drivers in Justiniano et al. (2010, 2011). To do this, we follow the procedure described in Forni *et al.* (2023), which identifies shocks according to their contribution to the cyclical variances of key variables.

Consider the structural representation of equation (4). The cyclical variance-covariance matrix of all variables in $\boldsymbol{Y_t}$ in the frequency band between $[\underline{\boldsymbol{\theta}}, \overline{\boldsymbol{\theta}}]'$ is given by:

$$\boldsymbol{V(\underline{\theta}, \overline{\theta}) = \int_{\underline{\theta}}^{\overline{\theta}} D(e^{-i\omega})D(e^{i\omega})'d\omega} \tag{7}$$

where, for example, in the case of business cycle frequencies $[\underline{\boldsymbol{\theta}}, \overline{\boldsymbol{\theta}}]' = [\boldsymbol{2\pi/32, 2\pi/6}]$ and $\boldsymbol{i}$ is the imaginary constant $\boldsymbol{i} = \sqrt{\boldsymbol{-1}}$. In practice, $\boldsymbol{V(\underline{\theta}, \overline{\theta})}$ can be obtained by computing the average over a grid of values between $\underline{\boldsymbol{\theta}}$ and $\overline{\boldsymbol{\theta}}$ and taking the real part of this average (or computing the inverse Fourier transform of the right-hand side in the above equation). This returns the total variation of all variables in $\boldsymbol{Y_t}$ in the given frequency band as the diagonal elements of the matrix $\boldsymbol{V}(\underline{\boldsymbol{\theta}}, \overline{\boldsymbol{\theta}})$.

To identify a particular shock instead, we use a single column $\boldsymbol{h}$ of the orthonormal matrix $\boldsymbol{H}$ to obtain:

$$\boldsymbol{\Psi}(\underline{\boldsymbol{\theta}}, \overline{\boldsymbol{\theta}}) = \int_{\underline{\boldsymbol{\theta}}}^{\overline{\boldsymbol{\theta}}} \mathbf{D}(\mathbf{e}^{-\mathbf{i}\boldsymbol{\omega}})\mathbf{h}\mathbf{h}'\mathbf{D}(\mathbf{e}^{\mathbf{i}\boldsymbol{\omega}})'\mathbf{d}\boldsymbol{\omega} \quad \mathbf{(8)}$$

which is the variation of all variables in the given frequency band stemming from the shock associated with column $\boldsymbol{h}$. For our identification strategy, we want to target only specific variables in a given band, so we select the rows of $\boldsymbol{D}$ that correspond to these variables. Suppose, for example, TFP is ordered second in $\boldsymbol{Y_t}$ then $\boldsymbol{D_m}$ for $\boldsymbol{m} = \mathbf{2}$ would select the corresponding row. As shown in Forni et al. (2023), this can easily be extended for multiple targets. This is discussed in more detail for the case of temperature shocks where we make use of this technique. We want to find the shock which contributed the majority of fluctuations in the given band to our target variable, so the column $\boldsymbol{h}$ is identified as:

$$\boldsymbol{h} = \mathbf{arg}\max_{\boldsymbol{h}} \left\{ \int_{\underline{\boldsymbol{\theta}}}^{\overline{\boldsymbol{\theta}}} \boldsymbol{D_m}(\boldsymbol{e}^{-\boldsymbol{i\omega}})'\boldsymbol{D_m}(\boldsymbol{e}^{\boldsymbol{i\omega}})\boldsymbol{d\omega} \right\} \text{ s.t. } \boldsymbol{h}'\boldsymbol{h} = \mathbf{1} \quad \mathbf{(9)}$$

The $\boldsymbol{h}$ that solves this is the unit-length eigenvector corresponding to the largest eigenvalue of the matrix sandwiched in between $\boldsymbol{h}$' and $\boldsymbol{h}$ in the above equation (as shown for the time domain in Uhlig, 2003).

We first identify the technology shock as the main driver of low-frequency variation in TFP as in Dieppe *et al.* (2021), which echoes the idea of Gali (1999) to identify technology shocks as the only long-run driver of labor productivity. Maximization does not imply that a single source is responsible for all long-run variation of TFP, but picks out the disturbance that contributes the most to its fluctuations. Dieppe *et al.* (2021) show this method to be more robust to interference from other shocks that typically occurs in variance maximization approaches such as Barsky and Sims (2011). Conditional on the identified technology shock, we then proceed to identifying the investment shock as the main driver of aggregate investment over the business cycle. Justiniano *et al.* (2010, 2011) show that such a shock can be interpreted as a shock to the marginal efficiency of capital, that is, how easily investment is converted to productive capital. The shock typically induces positive co-movement between investment and consumption in both representative and heterogeneous agent models (Auclert *et al.*, 2020). The conditional shock is identified by finding another column of $\boldsymbol{H}$ call it $\boldsymbol{h_j}$:

$$\boldsymbol{h_j} = \mathbf{arg}\max_{\boldsymbol{h_j}} \left\{ \int_{\underline{\theta}}^{\overline{\theta}} \boldsymbol{D_m}(\boldsymbol{e}^{-i\omega})' \boldsymbol{D_m}(\boldsymbol{e}^{i\omega}) \boldsymbol{d\omega} \right\} \text{ s.t. } \boldsymbol{h}'_{\boldsymbol{tech}} \boldsymbol{h_j} = \mathbf{0} \text{ and } \boldsymbol{h}'_{\boldsymbol{j}} \boldsymbol{h_j} = \mathbf{1} \quad \mathbf{(10)}$$

Finally, the labor supply shock is identified similarly to the TFP shock as the main driver of hours worked in the low frequency, but conditional on both the technology shock and the investment shock. This identification is inspired by Shapiro and Watson (1988) with an analogy to the relationship between Dieppe *et al.* (2021) and Gali (1999). It is easy to extend the maximization constraints in the above equation to pin down this labor supply shock.

To check whether our approach delivers valid identification, we study it in a controlled experiment using the model of Justiniano *et al.* (2011). The approach correctly recovers the true IRFs to the economic shocks in the majority of cases as reported in the Appendix. Moreover, we check if the sequence of conditional identifications matters for the results in a robustness exercise.

3.2.2. Identification of temperature shocks

We use a similar method as for the economic shocks to identify temperature shocks. Conditional on the three economic drivers, we extract the maximizers of temperature fluctuations in our data set. Economic theory can inform the identification of economic shocks, whereas there is no clear guideline for the identifying traits of climate-related shocks. For example, zero restrictions using a recursive (Cholesky) or long-run neutrality (Blanchard-Quah) scheme seem appropriate, as these would have to hold at every temperature location in our data set, requiring an impossible number of zero responses to be enforced. Maximizing frequency variations of temperatures has the advantage of being statistically driven rather than theoretically and allows us to target many temperature series simultaneously rather than restricting individual variables.

To do this, we need to extend the above framework slightly. Call the IRFs of the temperature variables $\boldsymbol{\Omega(L)} = \boldsymbol{\Lambda C(L) S}$ and collect the columns of $\boldsymbol{H}$ which identify the economic shocks in $\boldsymbol{H_E} = [\boldsymbol{h_{tech}}, \boldsymbol{h_{inv}}, \boldsymbol{h_{lab}}]$. Then the maximization program is the following:

$$\boldsymbol{h_{Tj}} = \mathbf{arg}\max_{\boldsymbol{h_{Tj}}} \left\{ \int_{\underline{\theta}}^{\overline{\theta}} \boldsymbol{\Omega_m}(\boldsymbol{e}^{-i\omega})' \boldsymbol{W}\, \boldsymbol{\Omega_m}(\boldsymbol{e}^{i\omega}) \boldsymbol{d\omega} \right\} \text{ s.t. } \boldsymbol{h}'_{\boldsymbol{Tj}} \boldsymbol{H_E} = [\mathbf{0}, \mathbf{0}, \mathbf{0}]' \text{ and } \boldsymbol{h}'_{\boldsymbol{Tj}} \boldsymbol{h_{Tj}} = \mathbf{1} \mathbf{(11)}$$

As before, $\boldsymbol{h_{Tj}}$ is a single column of $\boldsymbol{H}$ and can be found as the eigenvector of the matrix in the quadratic form in the above equation. $\boldsymbol{W}$ is a diagonal weighting matrix which contains the reciprocals of the square roots of the variances of the $\boldsymbol{m}$ targeted variables in the frequency band of interest. Given that all our data is measured in degrees Celsius, this is less of a concern, but is done for completeness.

We do not require the temperature shocks to be orthogonal to each other, only to the economic shocks, and inspect the resulting IRFs case by case. This is because the main identifying property these shocks have come from geography, which are hardly exclusive. Temperature fluctuations on the US west coast, for example, may be driven by additional impulses elsewhere in the country. Requiring these impulses to be orthogonal appears too restrictive. The targets and bands for identification are chosen as follows:

I. Maximize the low frequency temperature variation everywhere
II. Maximize the full spectrum temperature variation everywhere
III. Maximize the full spectrum temperature variation for the West coast (states that border the Pacific Ocean)
IV. Maximize the full spectrum temperature variation for the East Coast (states that border the Atlantic Ocean)
V. Maximize the full spectrum temperature variation for the Gulf of Mexico states (Texas, Louisiana, Mississippi, Alabama, Florida)
VI. Maximize the full spectrum temperature variation for non-coastal states
VII. Maximize the business-cycle spectrum temperature variation everywhere to capture the ENSO pattern
VIII. Maximize the high-frequency temperature variation everywhere to capture the weather shock predominantly used in the literature

The choice is motivated by the geographical patterns we observe in the data, which suggest important temperature commonalities in the Midwest, on the coastal regions, and the Gulf area. Moreover, the maximizer of low frequency temperature movements will likely pick up some non-US socio-economic shocks, and the full-spectrum maximizer is the closest to the temperature shock measured in an approach that uses average temperatures, only in this case, it is purged of US economic activity.

It is important to point out two properties of the shocks that are identified in our FAVAR framework. First, the shocks induce deviations of temperatures at many geographical locations in the US from their deterministic components. If the deterministic component of temperatures contains any trending behavior, a temperature shock constitutes a deviation from this trend. In that sense, explicitly computing the deviation of temperatures from some long-term trend and then using these deviations as a shock, as is done in Kahn et al. (2021), for example, is very similar, but skips the identification step that tries to pinpoint if the deviation comes from human sources or is of natural causes. Second, some climate econometric research stresses the importance of extreme weather events as more suitable measures of temperature shocks (Natoli, 2023). The shocks that we construct are precisely this: they are not predictable from past information about temperatures anywhere in the contiguous US and neither from information about GDP, TFP, investment, or hours worked. Whether this information set is sufficient is a difficult question to answer. Moreover, non-linearities or state-dependence may play an important role in the transmission of such shocks, all of which we consider to be important avenues for future research.

4. Results

4.1. Descriptive results

We begin by summarizing the linkages between the US economy and temperatures through the lens of the model in equations (1) and (2). As a first exercise, we determine the number of shocks that drive US temperatures. In the macroeconometric literature, such shocks are sometimes referred to as deep shocks (Forni *et al.*, 2009). We do this by maximizing the full-spectrum fluctuations of all US temperature series without conditioning on other shocks. Notice that this is done on the spectral density matrix rather than the sample correlation matrix used for the computation of the principal components. We repeat the same exercise and target the full spectrum of variation in the four economic variables to see how these shocks affect temperatures. The outcomes of this are reported in Tables 2 and 3.

TABLE 2 • CUMULATIVE CYCLICAL VARIANCES EXPLAINED BY THE FIRST SIX SHOCKS THAT MAXIMIZE THE FULL SPECTRUM VARIATION OF TEMPERATURES AT GRID-CELL LEVEL IN THE US. ROUNDED TO TWO DECIMALS

	Low Frequencies						Business Cycles						High Frequencies					
	1	2	3	4	5	6	1	2	3	4	5	6	1	2	3	4	5	6
Avg. Temp.	0.3	0.48	0.58	0.78	0.83	0.87	0.42	0.63	0.78	0.81	0.87	0.92	0.42	0.65	0.77	0.8	0.86	0.92
GDP	0	0.01	0.01	0.07	0.08	0.12	0	0.01	0.01	0.19	0.22	0.27	0.01	0.02	0.02	0.08	0.09	0.12
TFP	0	0.04	0.06	0.23	0.27	0.28	0	0.03	0.07	0.52	0.59	0.6	0.01	0.02	0.04	0.29	0.3	0.31
Hours	0	0.01	0.01	0.08	0.1	0.14	0	0.01	0.02	0.25	0.31	0.36	0.02	0.03	0.05	0.18	0.2	0.22
Investment	0	0.02	0.02	0.04	0.06	0.08	0.01	0.01	0.02	0.13	0.16	0.2	0	0.01	0.03	0.06	0.07	0.09

TABLE 3 • CUMULATIVE CYCLICAL VARIANCES EXPLAINED BY THE FIRST SIX SHOCKS THAT MAXIMIZE THE FULL SPECTRUM VARIATION OF GDP, TFP, HOURS, AND INVESTMENT IN THE US. ROUNDED TO TWO DECIMALS

	Low Frequencies						Business Cycles						High Frequencies					
	1	2	3	4	5	6	1	2	3	4	5	6	1	2	3	4	5	6
Avg. Temp.	0.03	0.22	0.31	0.33	0.4	0.47	0.01	0.02	0.05	0.06	0.14	0.24	0.01	0.02	0.03	0.04	0.1	0.2
GDP	0.93	0.96	1	1	1	1	0.71	0.84	0.91	0.99	0.99	0.99	0.78	0.83	0.87	0.93	0.93	0.97
TFP	0.57	0.96	1	1	1	1	0.17	0.83	0.92	0.98	1	1	0.42	0.78	0.84	0.91	0.95	0.97
Hours	0.78	0.98	0.99	1	1	1	0.43	0.96	0.96	0.99	1	1	0.34	0.85	0.88	0.94	0.96	0.98
Investment	0.88	0.94	0.97	1	1	1	0.53	0.75	0.76	0.99	1	1	0.44	0.54	0.55	0.9	0.93	0.99

Two important new findings emerge from these tables. First, the common variation in US temperatures requires at least five shocks to reach more than 80% explained cyclical variance at all frequencies. After the fifth shock, the improvement in explained variance in any of the three bands of interest from adding another shock is below 5%. This number constitutes a lower bound for the actual number of exogenous temperature drivers, as the shocks here are not structurally identified, other than being mutually orthogonal variance maximizers. Based on this result, reducing the effects of temperatures on economic aggregates to a single variable such as a (weighted) average, as is frequently done in the literature, is implausible.

Second, there is a connection between temperature and economic variation, mostly through TFP. The fourth temperature variance maximizer is responsible for a sizable share of TFP variation at all frequencies, particularly at the medium part of the spectrum. This seems intuitive: the low and medium frequencies are related to the trend in the temperature data and it is commonly believed that anthropological forces have contributed to this trend in the past half century. Since technology is an important ingredient for economic growth, we should expect it to correlate with the lower frequency components of temperatures. Moreover, we observe that, in line with the literature (e.g., Forni *et al.* (2023)), two shocks appear sufficient to capture a large share of the cyclical variation in key aggregate economic variables. In the low frequency and business cycle bands, hours, investment, and GDP are largely driven by the same shock, yet TFP is not. This echoes the findings of Angeletos *et al.* (2020) who also demonstrate a disconnection between TFP and business cycle fluctuations of GDP. Interestingly, investment fluctuations of high frequency appear to require more than three shocks to be accurately explained. Finally, we see that the second shock, which especially drives long-run TFP, is responsible for a large increase in the explained variance of average US temperatures.

The descriptive exercise does not allow us to tell apart the respective source of the fluctuation. Is the variation in temperatures due to climatic or economic shocks? What part of GDP variation is truly due to climatic shocks and which part just masquerades as interference from economic shocks? These questions go back to the cyclical nature of the climate-economic system, and we need the structural identification exercise explained in the preceding section for an answer.

4.2. Semi-structural results

4.2.1. Economic shocks

We begin by discussing the effects of the economic shocks on the economic variables. This is done to confirm that our identification procedure is indeed successful in selecting technology, labor supply, and investment related shocks as described in the macroeconomic literature. The impulse response functions for this are reported in Figure 4.

FIGURE 4 • IMPULSE RESPONSE FUNCTIONS FOR THE THREE STRUCTURAL ECONOMIC SHOCKS
Shaded areas are bootstrapped 68% and 90% confidence bands

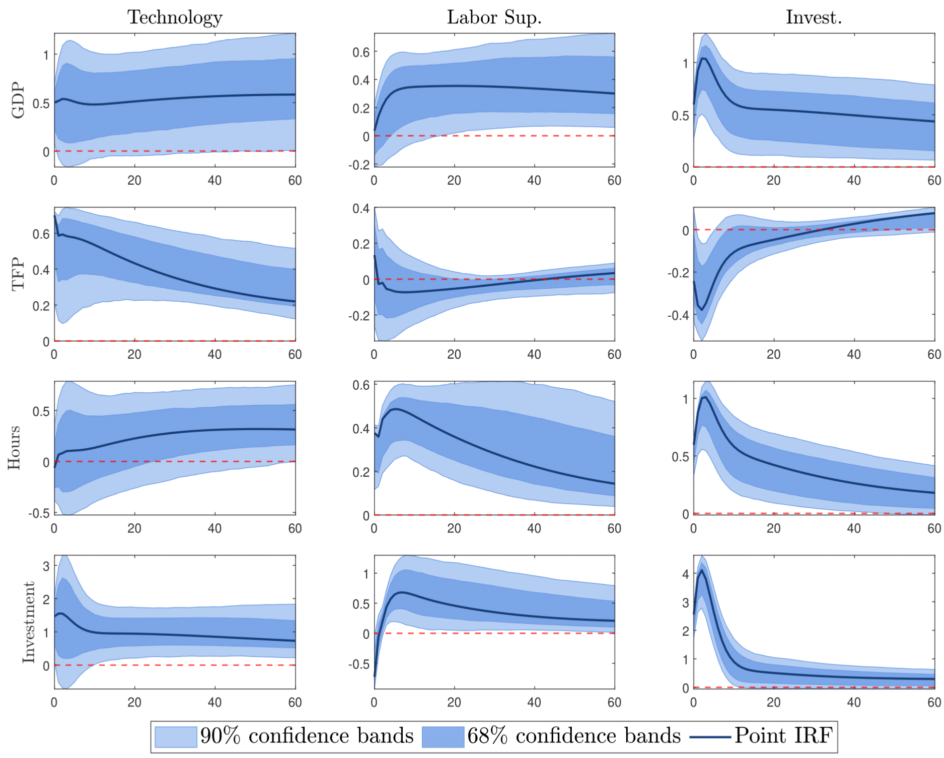

First, the technology shock leads to an immediate increase in TFP which is accompanied by an expansion of real GDP of around 0.4%. Hours initially decline (although this is statistically insignificant) and investment increases. These results are very similar to those found in Dieppe *et al.* (2021), who use labor productivity in a spectral identification exercise with a different VAR specification.

Second, the labor supply shock leads to a slowly-building increase in output of around 0.3%, a mildly hump-shaped response of hours after an initial increase, and an initial reduction in investment which is replaced by labor as an input to production. The TFP response is almost entirely insignificant, which is partially a result of conditioning on the technology shock. The slow-building GDP response is consistent with other studies that identify labor supply shocks such as Foroni *et al.* (2018) (for the US) and Peersman and Straub (2009) (for the euro area). The responses of hours and GDP are in line with the paper of Shapiro and Watson (1988), which we have used as motivation for the identification strategy.

Lastly, the investment shock creates hump-shaped expansions in investment, hours, and GDP and a hump-shaped decline in TFP. These responses are in line with the motivating paper of Justiniano *et al.* (2011). The decrease in TFP is also observed in Ben Zeev and Khan (2015) (although in their paper the response is insignificantly different from zero) for investment-specific technology shocks. More inputs are used to produce only slightly more output, thus productivity must fall. We take these results as evidence that our proposed identification strategy can indeed correctly pick out empirically valid impulse responses in a joint identification framework, even though the identification approach is entirely built on spectral identification and does not exactly copy the approaches in the originally proposed papers.

Next, we describe the responses of US temperatures to the three expansionary economic shocks, a key result of this paper. It is important to note that the impact reactions (near impulse response horizon $\boldsymbol{h = 0}$) of temperatures across the US to the shocks are difficult to measure accurately due to the high volatility of the temperature time series as opposed to the macroeconomic aggregates. We therefore prefer not to interpret temperature responses to economic shocks near the impact. The graphs in Figure 5 show the following picture: the technology shock has a cooling effect on temperatures in the east and the south of the US. Importantly, as the impulse horizon increases, the effect dissipates almost everywhere, which suggests that eventually, cooling and warming offset each other. The effect is persistently significant at the 68% confidence level even after 10 years. The investment shock leads to increases in temperatures almost throughout the US after 10 years, initially dominating in California, Arizona, near the Canadian border, and in the east. Finally, a similar pattern emerges for the labor supply shock, although the initial temperature responses are less pronounced compared to the investment and technology shocks. As far as the magnitudes of the responses are concerned, they range between –0.03 and 0.01°C (technology shock), -0.01 and 0.02°C (labor supply shock), and –0.01 and 0.02°C (investment shock).[2]

[2] These values are computed across all horizons and grid cells as a single standard deviation around the mean response for each of the three shocks.

FIGURE 5 • GRID CELL TEMPERATURE IRFS AT GIVEN HORIZONS IN RESPONSE TO THE THREE ECONOMIC SHOCKS

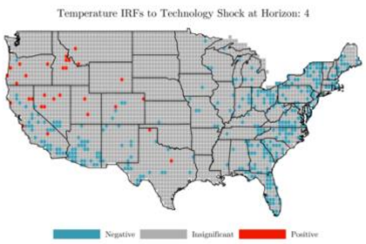

a) Tech. shock after 1 year

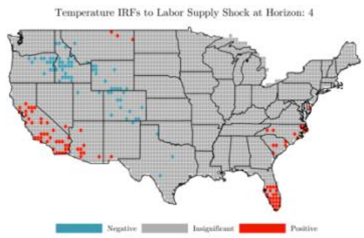

b) Lab. Sup. shock after 1 year

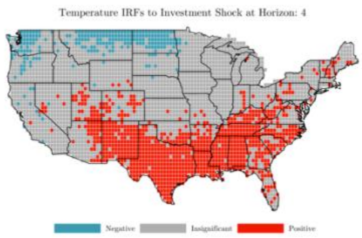

c) Inv. shock after 1 year

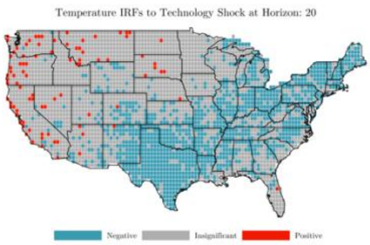

d) Tech. shock after 5 years

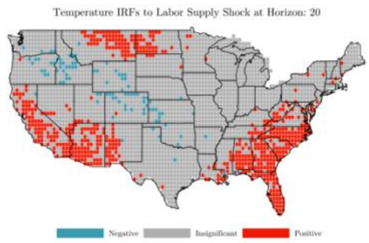

e) Lab. Sup. shock after 5 years

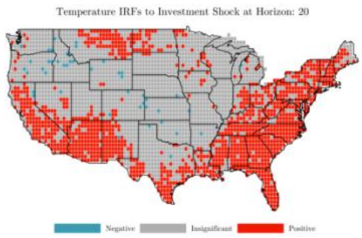

f) Inv. shock after 5 years

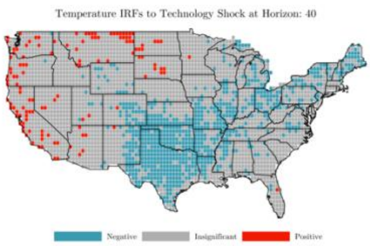

g) Tech. shock after 10 years

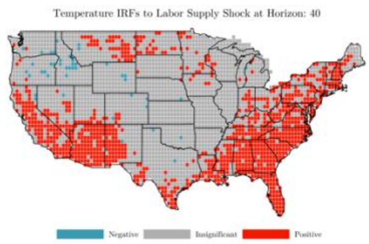

h) Lab. Sup. shock after 10 years

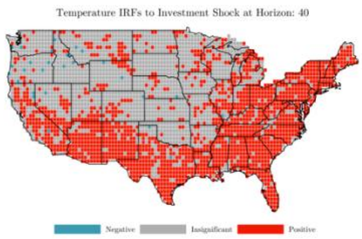

i) Inv. shock after 10 years

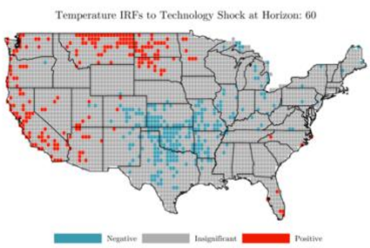

j) Tech. shock after 15 years

k) Lab. Sup. shock after 15 years

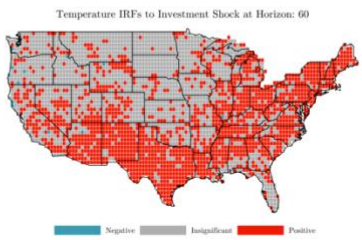

l) Inv. shock after 15 years

Next, in Table 4 we report the relative importance of each of the three economic shocks in explaining average temperature movements, as well as the fluctuations of our economic variables at low, business cycle, and high frequencies.

TABLE 4 • INDIVIDUAL CYCLICAL VARIANCES EXPLAINED BY THE THREE IDENTIFIED ECONOMIC SHOCKS OVER THE THREE FREQUENCY BANDS
Numbers in parentheses are the 90% confidence bands associated with the percentage above. Rounded to two decimals

	Low Frequencies			Business Cycles			High Frequencies		
	Tech.	Lab. Sup.	Invest.	Tech.	Lab. Sup.	Invest.	Tech.	Lab. Sup.	Invest.
Avg. Temp.	0.1	0.04	0.11	0.01	0.01	0.01	0.01	0.01	0
	(0.04,0.36)	(0.04,0.19)	(0.05,0.22)	(0.01,0.06)	(0.01,0.06)	(0.02,0.07)	(0.01,0.05)	(0.01,0.05)	(0,0.03)
GDP	0.46	0.13	0.34	0.24	0.05	0.58	0.46	0.04	0.36
	(0.04,0.93)	(0.01,0.47)	(0.02,0.58)	(0.04,0.75)	(0.01,0.21)	(0.13,0.73)	(0.11,0.79)	(0.01,0.26)	(0.06,0.54)
TFP	0.84	0.02	0.08	0.57	0.02	0.28	0.7	0.07	0.09
	(0.62,0.99)	(0,0.16)	(0,0.15)	(0.14,0.83)	(0.01,0.27)	(0.04,0.46)	(0.19,0.72)	(0.01,0.29)	(0.02,0.21)
Hours	0.32	0.24	0.44	0.04	0.14	0.79	0.13	0.24	0.54
	(0.06,0.83)	(0.07,0.5)	(0.04,0.65)	(0.02,0.53)	(0.03,0.21)	(0.26,0.82)	(0.07,0.59)	(0.04,0.29)	(0.14,0.56)
Investment	0.52	0.08	0.39	0.1	0.03	0.85	0.21	0.11	0.56
	(0.11,0.89)	(0.01,0.33)	(0.06,0.64)	(0.02,0.51)	(0.01,0.07)	(0.42,0.92)	(0.06,0.42)	(0.01,0.16)	(0.26,0.66)

Taken together, the three economic shocks explain around 25% of the low-frequency movement of temperatures. Technology and investment shocks contribute the most (10% and 11%, respectively), while labor supply shocks contribute less (4%). We conclude from this that a non-negligible share of the trend- and long-cycle component of temperatures is caused by anthropological activity in the United States. The economic shocks are not important sources of average short-term temperature fluctuations, which we interpret as evidence that such fluctuations are mostly due to natural or non-US causes. The three shocks also appear to be reasonable choices to explain business cycle fluctuations in the economy. Together, they account for 87% of the business cycle (BC) variation in GDP, 87% of the variation in TFP, 97% of the variation in hours, and 89% of the variation in investment.

The spatial distribution of explained variances for the three shocks is presented in Figure 6. Given that there is hardly any variance arising at medium and short frequencies, we report this only for the low frequency. Patches of relevant fluctuations are observable in all three cases. For the technology shock, the variances explained are around 35% in the east and in the south, particularly in Texas. For the investment and labor supply shocks, the patterns emerge predominantly in the south and in the corridor across Colorado, Wyoming, and Idaho, where the labor supply shock was cooling. Explained variances for the investment shock are locally larger than 40% in some areas in the south, while they are lower in the case of the labor supply shock.

FIGURE 6 • GRID CELL LEVEL CYCLICAL VARIATION EXPLAINED AT LOW FREQUENCIES FROM THE THREE ECONOMIC SHOCKS

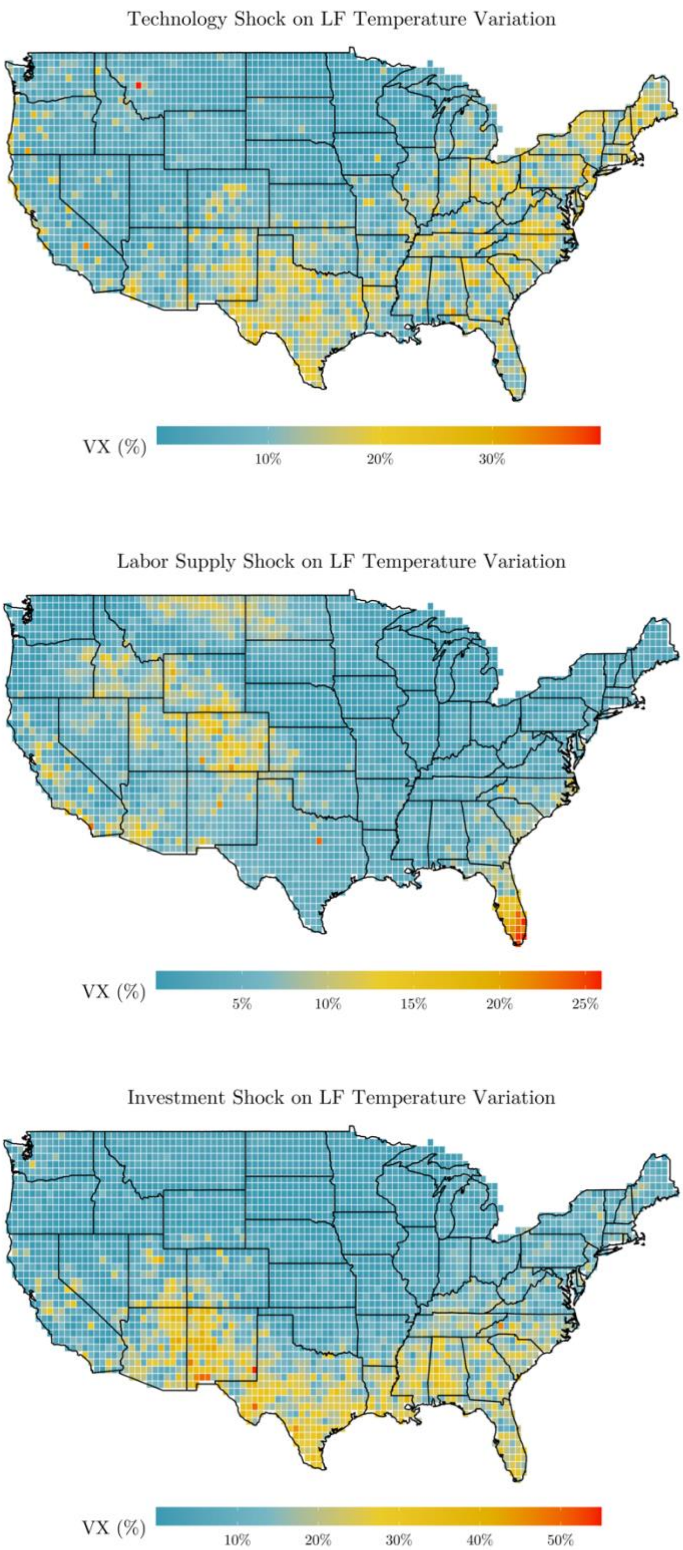

4.2.2. Temperature shocks

Next, we turn to the effects of the temperature shocks that are identified as described in section 3. For ease of interpretation we have normalized all shocks such that the impact response in average temperatures is scaled to 1 degree Celsius, as is customary. We are primarily concerned with the effect of temperature changes on GDP as all other economic variables were used for identification purposes. Figure 7 summarizes the resulting IRFs.

FIGURE 7 • IMPULSE RESPONSE FUNCTIONS FOR THE DIFFERENT TEMPERATURE SHOCKS. Shaded areas are bootstrapped 68% and 90% confidence bands

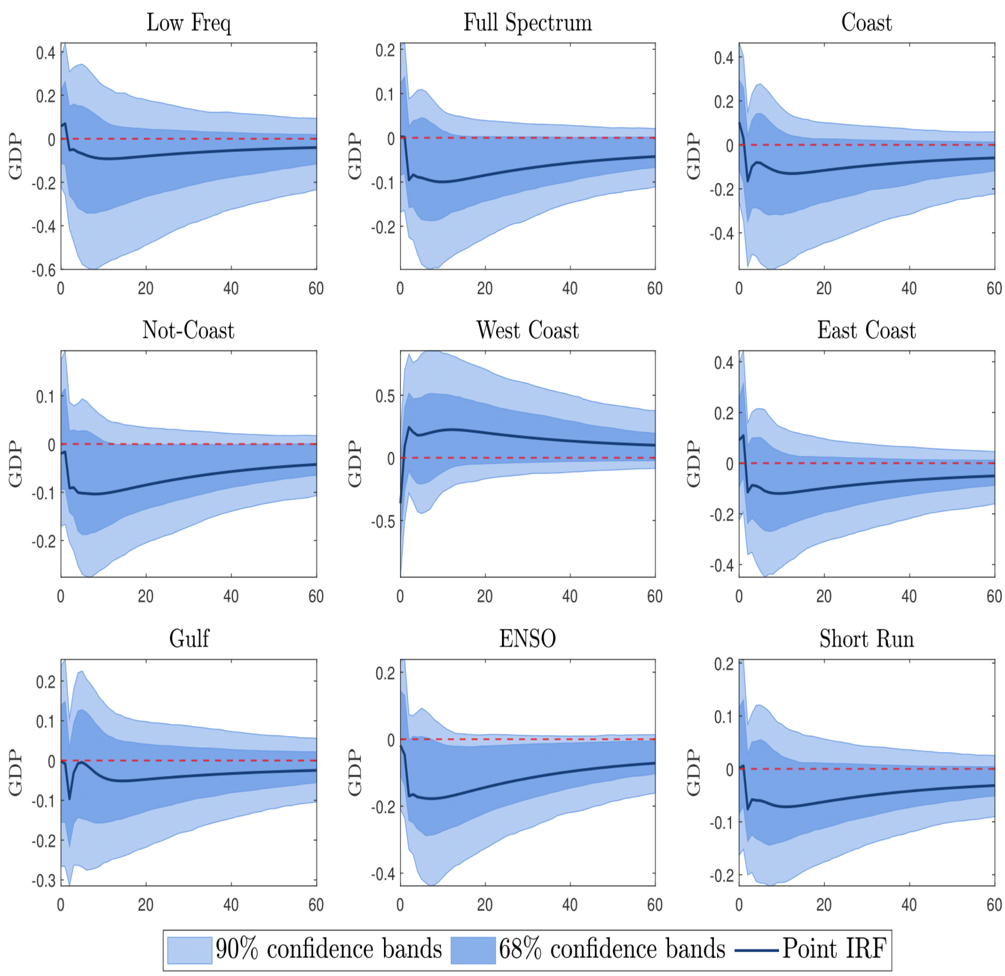

All of the identified shocks lead to small and persistent GDP contractions between 0.1% and 0.2%, except for the shock that primarily affects the West Coast of the US. The confidence bands are consistently very close to the zero line. This result aligns with the majority of the literature, which finds substantial uncertainty in the estimates of temperature shocks in the US. For example, Newell *et al.* (2021) and Nath *et al.* (2023) find nearly zero effects for countries with an average temperature around 13 degrees Celsius, such as the

US. Negative effects of temperature shocks in the range of 0.1% are also reported by Natoli (2023) (although using an instrumental variable approach), and slightly more negative impacts are documented by Colacito *et al.* (2019). Dell *et al.* (2012) found insignificant effects of temperatures on output in rich countries. These results are consistent with the shock in our set that maximizes temperature variation across the entire US over all frequency bands. However, our analysis goes beyond this conclusion, revealing that more than one shock is needed to capture US temperature variation. In fact, without imposing orthogonality for this exercise, the West Coast shock is only 2% correlated with the low-frequency maximizer, 3% with the full spectrum maximizer, and a relatively low 33% with the East Coast shock. Interestingly, it produces a comparatively sizable expansion in aggregate GDP (although this is statistically insignificant). This effect would either be lost entirely or blended into average results obtained through conventional econometric techniques. As Table 4 suggests, the share of variation in the economic variables from temperature movements is very small, which is why we choose not to report them here.

For illustration of the spatial distribution of impulse responses, we focus on the full spectrum maximizer for temperatures everywhere and the West Coast shock. These two shocks are only 3% correlated, without the imposition of orthogonality. Figure 8 shows the signs of the responses. Clearly, the full spectrum maximizer without geographical constraints raises temperatures everywhere except for the West Coast. The shock that drives temperatures up on the West Coast simultaneously decreases them in the East. Due to the scaling of the average temperature to equal 1°C, the positive responses outweigh the negative ones. Both of these shocks are quantitatively important for temperature variations (38% and 16% on average, respectively, over all frequency bands). Importantly, we find no evidence of significant persistence in either of the temperature shocks considered here. After around three years, all effects on temperatures turn insignificant.

FIGURE 8 • GRID CELL TEMPERATURE IRFS AT GIVEN HORIZONS IN RESPONSE TO THE FULL SPECTRUM AND THE WEST COAST TEMPERATURE SHOCKS

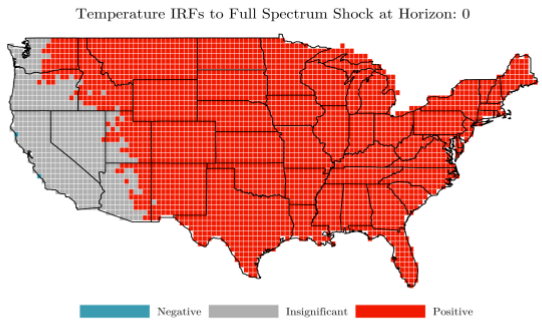

a) Full spectrum shock on impact

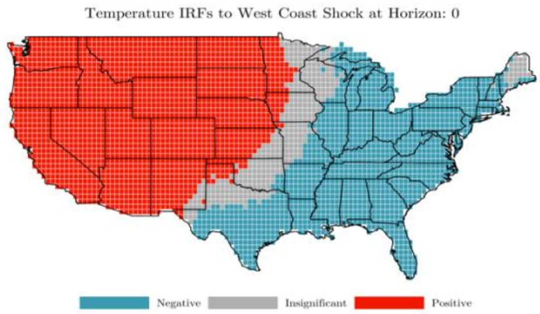

b) West coast shock on impact

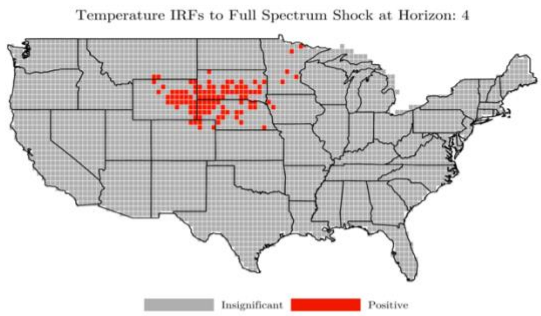

c) Full spectrum shock after 1 year

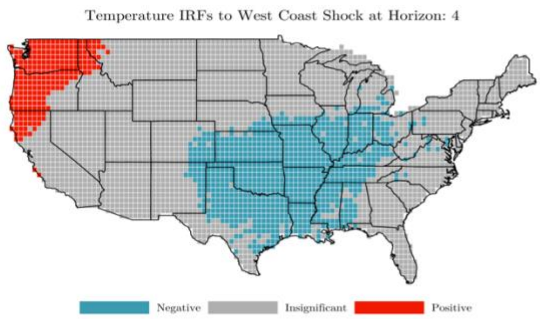

d) West coast shock after 1 year

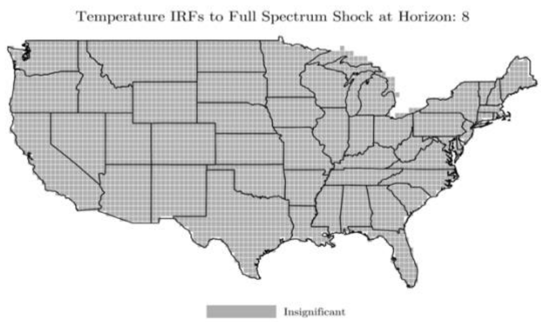

e) Full spectrum shock after 2 years

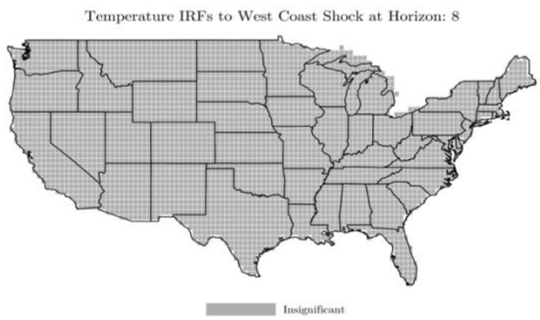

f) West coast shock after 2 years

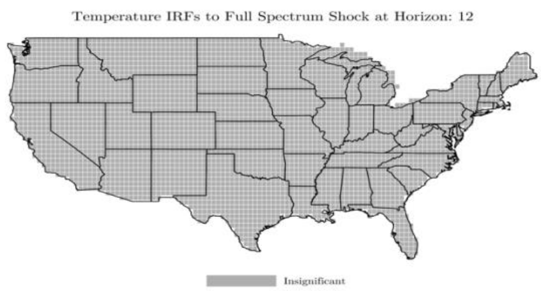

g) Full spectrum shock after 3 years

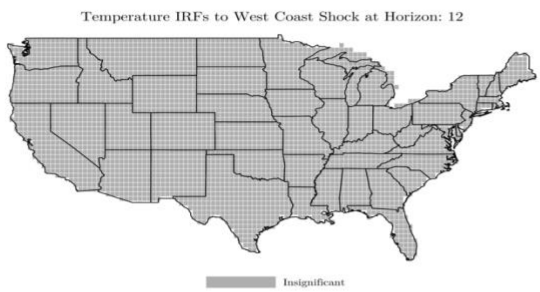

h) West coast shock after 3 years

To summarize the semi-structural results, we observe that economic sources, particularly technology and investment shocks, are locally important drivers of temperature variations. These shocks lead to noticeable decreases (technology) and increases (investment, labor supply) in temperatures that persist for many years and are noticeable even relatively shortly after the initial shock. Treating temperatures as unaffected by anthropogenic forces even in the short run can thus lead to confounding causal effects, especially when annual data is used, as is customary in the literature. Moreover, it is crucial to distinguish the effects of temperature shocks on aggregate GDP based on the geographical location of the shock's epicenter. If the West Coast is predominantly affected, GDP may remain unaffected or even increase, while shocks in other parts of the country can lead to small contractions. This distinction is important for assessing the damages of temperature warming, which are incorporated into models used for policy decisions.

5. Discussion

5.1. The effects of economic shocks on temperatures

The documented effects of the three economic shocks on temperatures across the US warrant closer inspection. The connection between economic activity and temperatures operates through the emission and storage of climate-active gases. Magnus *et al.* (2011) decompose the temperature effect of anthropogenic gas emissions into warming – through the emission of greenhouse gases (GHGs), most prominently CO_2 – and cooling – through aerosol emissions, most prominently SO_2. CO_2 is a long-lived, well-mixing gas that spreads through the Earth's atmosphere over time, while SO_2 produces quick but more short-lived localized cooling by reflecting incoming solar radiation.

There is increasing evidence from the natural sciences literature suggesting that emission impulses can lead to temperature effects within a short time span. Notably, Ricke and Caldeira (2014) and Zickfeld and Herrington (2015) suggest that CO_2 emission impulses can lead to significant warming relatively quickly – 93% of the peak warming effects materialize after 10-15 years following an emission impulse in their experiments, even considering potential non-linearities. Such horizons are well within the customary projection range for FAVAR models. Complementary to this, Joos *et al.* (2013) calculate average surface-temperature responses to CO2 emission impulses and find positive reactions contemporary with the initial impulse. Methane is another powerful GHG that develops much of its effects over a short horizon (Mar *et al.*, 2022). Therefore, our finding of quick temperature changes in the US after economic shocks aligns with results found in climatology research. Nevertheless, we want to emphasize that the very long run, where GHG effects are still active, may be less precisely estimated in our model.

Technology shocks induce cooling in parts of the US east and south. This suggests that the solar radiation effect from aerosol emissions outweighs the heating effect from GHG emissions at these locations, especially in the short run. We investigate this hypothesis further by running the following analysis: to the VAR consisting of GDP, TFP, investment, and hours worked, we add time series for GHGs and SO_2 emissions in the US for the same sample we used in our previous analysis. The emissions data are available at a yearly frequency. The data for GHGs are retrieved from https://ourworldindata.org/greenhouse-gas-emissions and are based on Jones *et al.* (2023); the data for SO_2 are from Smith et al. (2011) until 1990 and from then on from the EPA (https://www.epa.gov/air-emissions-inventories/air-pollutant-emissions-trends-data). We estimate the VAR with a single lag and identify a technology shock and an investment shock in exactly the same fashion as before, using frequency domain techniques.

FIGURE 9 • IMPULSE RESPONSE FUNCTIONS OF LOG EMISSIONS TO TECHNOLOGY AND INVESTMENT SHOCKS IN THE YEARLY VAR (1) FOR ONLY ECONOMIC VARIABLES.
Identification in the frequency domain adapted to yearly measurements

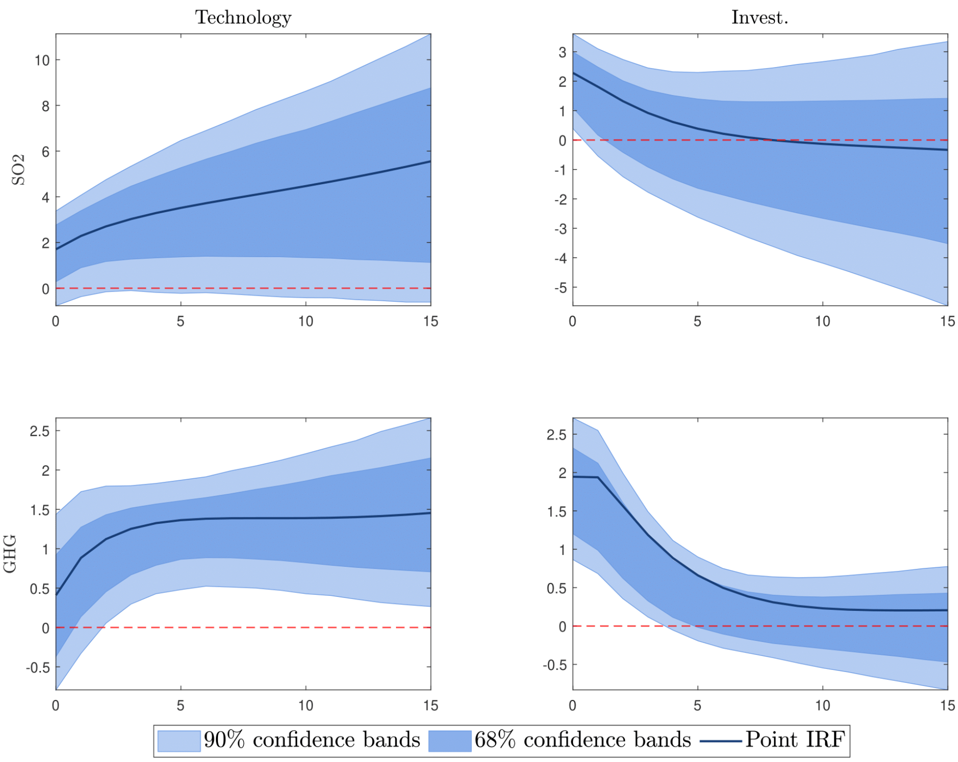

Figure 9 shows the responses of SO_2 and GHG emissions to the two main expansionary shocks (technology and investment). The impulse response functions (IRFs) for the other economic variables are consistent with the quarterly exercise and are therefore not reported again. The permanent shock to TFP also leads to permanent increases in both SO_2 and GHG emissions. However, the increase in SO_2 emissions is about 2% initially and up to 6% after 15 years, while GHG emissions increase only between 0.5% on impact and slightly below 1.5% in the long run. We interpret this as evidence that what we observe in the quarterly FAVAR is cooling from increased aerosol emissions. This observation is consistent with the localized effects in the south-east of the country, which we discuss further below. Importantly, as noted in Magnus *et al.* (2011), SO_2 is itself short-lived. Despite the sustained increase in SO_2 emissions, the cumulative warming effect from GHGs eventually neutralizes the cooling from aerosols in our quarterly FAVAR, which is why, as the IRF horizon increases, the cooling effects disappear or even turn into warming. For the investment shock, on the other hand, we observe impulses in both SO_2 and GHGs of equal magnitude. However, the SO_2 impulse is only mildly significant for about one year before emissions (insignificantly) decrease. GHG emissions increase strongly and persist for a longer period, leading to the rapid dissipation of the cooling effect and dominance of the warming effect from GHGs throughout the horizon in the quarterly FAVAR. This explains why temperature changes after the investment shock are observed across almost the entire country and remain significant even after 15 years – there is no sustained counteracting cooling effect.

FIGURE 10 • SO_2 AND CO_2 EMISSIONS ARE COMPUTED FROM EPA'S NEI 2020 DATA SET FOR SITE-SPECIFIC EMISSIONS (https://www.epa.gov/air-emissions-inventories/2020-national-emissions-inventory-nei-data). These include emissions from fossil fuel combustion, industrial processes and biomass (e.g. Wildfires), but exclude *onroad* emissions

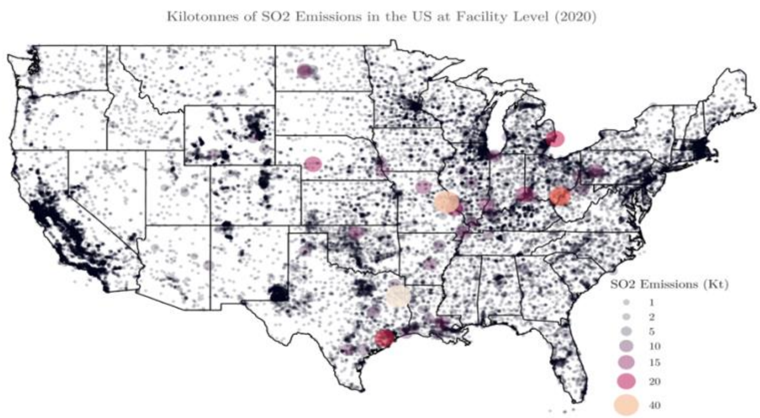

a) Sulfur dioxide emissions 2020

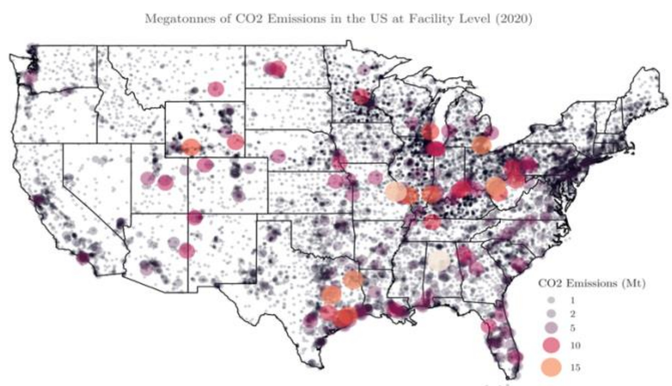

b) Carbon dioxide emissions 2020

Curiously, the geographical pattern of temperature changes following a technology shock, as shown in Figure 6, roughly coincides with the locations of important parts of the American energy-producing, manufacturing, and natural resource processing industries. Figure 10 demonstrates that these areas are also centers of CO_2 and SO_2 emissions. Conley *et al.* (2018) study the responses of temperatures to the hypothetical removal of all US-based SO_2 emissions and document a very similar geographical pattern (with inverted signs, as they consider SO_2 removal rather than emission). Based on this observation, we are confident that our economic shocks lead to temperature-altering emissions in the expected parts of the country. Furthermore, given the localized nature of aerosol-related cooling, we interpret this spatial pattern as evidence that the channel we identify for our technology shock is indeed dominated by SO_2 emissions.

5.2. The effects of temperature shocks on GDP

Next, we turn to the discussion of the different effects of west coast-centered temperature shocks and the other temperature shocks we have identified. We focus on the full spectrum maximizer as a representative of the other shocks and recall that both shocks lead to a one centigrade increase in average US temperatures, but the GDP responses present opposite signs. Our reasoning for this finding is based on previous results in the literature.

First, consider sector-level responses. Increases in temperatures have been shown to reduce output in almost every industry, especially in agriculture and construction (Colacito *et al.*, 2019). The temperature increase that follows the full spectrum shock affects almost the entire US and thus essentially all industries (a notable exception being California), thus depressing aggregate GDP. Conversely, the west coast shock leads to increased temperatures on the west coast but is accompanied in the data by lower temperatures in the east. In our linear model, decreasing temperatures should be beneficial for output in those states. The heating in the west does not appear to offset this positive effect.

Second, we turn to geographical differences. Hsiang *et al.* (2017) provide estimates of the projected spatial distribution of climate effects for the US. They calculate a gain in agriculture from increased temperatures in the north-west of the country and project overall total damages to concentrate in the south-east of the country, whereas the north-western states experience positive effects from warming. The largest damages from temperature increases go through excess mortality in the densely populated east and the already warmer south of the US in their study, also reported by Carleton *et al.* (2022). Therefore, the warming in the west and cooling in the east we document after the west coast shock should benefit the western industries and lead to fewer deaths in the east, which sums to a net positive effect for aggregate GDP. The full spectrum shock, on the other hand, does not produce the warming gains in the north-west but leads to warming in the areas where excess mortality has been shown to be of high importance in the transmission of temperatures to GDP.

In light of these arguments, we carry out the following exercise to better understand how the shocks impact state-level income. We expect the full spectrum shock to be damaging almost everywhere and the west coast shock to be expansionary, at least in the eastern states, but potentially also in the west. To do this, we run the following local projections (Jordà, 2005) for each state in the contiguous US individually:

$$y_{t+h} = \mu_h + \beta_h \widehat{s_t} + \gamma_h(L) y_{t-1} + \epsilon_{t+h}, \quad \text{for h} = 1, 2, \dots, 40 \tag{12}$$

where y_{t+h} is the log of quarterly real personal income,[3] μ_h is a constant, $\widehat{s_t}$ is alternatively the unit variance full spectrum or west coast shock estimated in the FAVAR, $\gamma_h(L)$ is a lag-polynomial of order two as in the FAVAR, and ϵ_{t+h} is a forecast error. The coefficient β_h measures the response to the shock of interest at each horizon h.

Figure 11 shows that the full spectrum temperature shock indeed decreases income in nearly all states, except for New York, which nonetheless experiences reductions in income for most of the horizon. The west coast shock, on the other hand, produces mixed impulse response functions (IRFs). The majority of economically large states (by share of national GDP) experience income increases, except for Colorado, Florida, and Texas, where the losses are relatively small. Big west coast economies such as California and Washington see long-run benefits from the shock, although these are small in magnitude. We take the evidence from this auxiliary model as supportive of the idea that temperature increases, in general, are detrimental for output, possibly by increasing mortality or lowering productivity. However, we caution that a measured increase of average US temperatures of one degree Celsius can come in different shapes, which produce different dynamics at the state level and then translate into different aggregate responses. We believe that our two example shocks are good representations of actual co-movement in temperatures experienced in the US. Any exercise focusing on the simple average temperature, which is similar to the full spectrum maximizer, will likely miss the effects induced by the west coast shock and may lead to incomplete conclusions for damage functions and policy implications.

[3] Personal income data at the state level at quarterly frequency is collected from BEA table SQINC4 and deflated using the GDP deflator and alternatively the CPI. The sample spans Q1:1948 - Q4:2017.

FIGURE 11 • IMPULSE RESPONSES TO THE FULL SPECTRUM AND THE WEST COAST TEMPERATURE SHOCKS IDENTIFIED IN THE FAVAR

IRFs are obtained by means of a local projection of real personal income at the state level onto its own lags and the identified unit variance shock. The states with name tags are the largest 15 states by GDP. Blue lines indicate negative responses after 40 quarters. Red lines indicate positive responses after 40 quarters

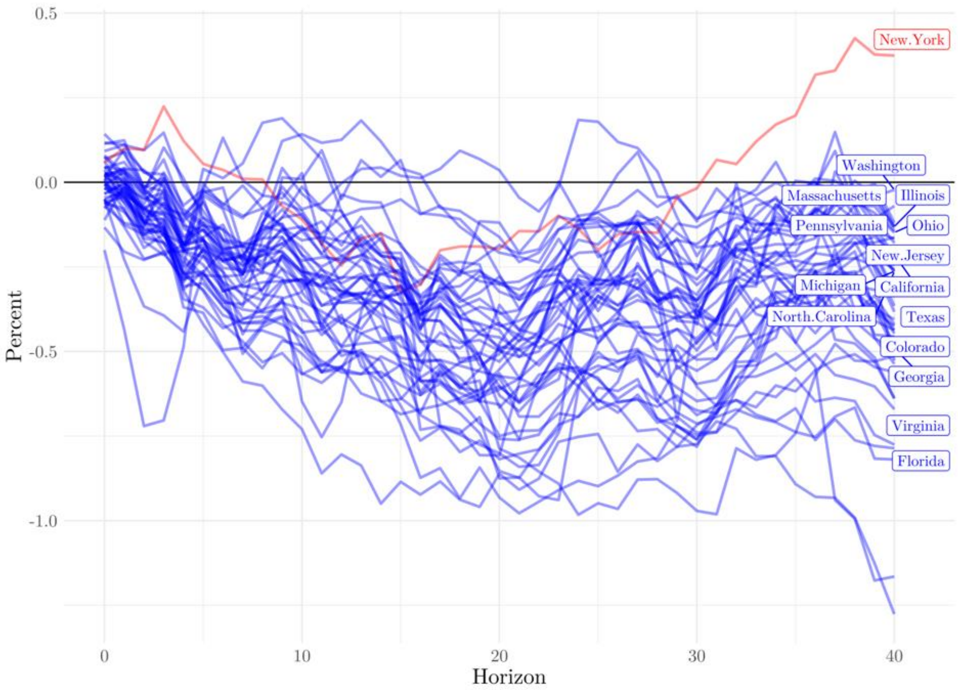

a) Full spectrum shock on real personal income

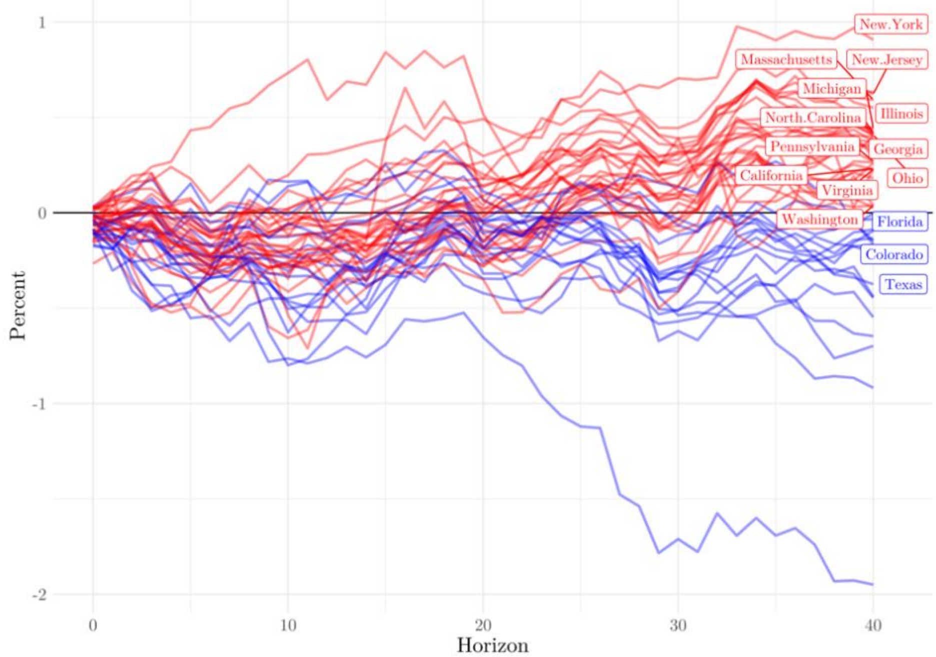

c) West coast shock on real personal income

6. CONCLUSION

We model an empirical joint climate-economic system to investigate the effect of economic shocks on temperatures in the US and vice versa. Using the principal components of a large, gridded dataset of US temperatures, we show that at least five shocks are necessary to accurately reflect temperature variations of different frequencies everywhere in the contiguous US, calling into question papers that use a single "climate shock" or focus on cross-sectional averages to reflect temperature warming. We show that a clear connection between the economy and temperatures exists, which is mostly driven by changes in Total Factor Productivity (TFP). We identify three economic shocks, arguably responsible for the bulk of business-cycle and long-term variation in the US economy and thus emissions of climate-active gases – a technology shock, a labor supply shock, and an investment shock. Identification in the frequency domain allows us to mix medium-term and long-term identification assumptions. There is clear evidence that economic activity has affected US temperatures. Together, the three shocks account for around 25% of the low-frequency component of US temperatures. Investment shocks increase temperatures on average, technology shocks decrease them, and we explore the reasons for this by showing a significant role for aerosol emissions that induce local, short-lived cooling and greenhouse gas (GHG) emissions that lead to slow-paced, encompassing warming.

On the other hand, the economic damages from changing temperatures are small and come with substantial uncertainty. We show that temperature changes that affect primarily the US west coast lead to small economic expansions, as they are accompanied by decreasing temperatures in the east and south. Shocks raising temperatures elsewhere are mildly recessionary, suggesting that the US has been well-adapted to temperature change in the past.

References

Acevedo, S., Mrkaic, M., Novta, N., Pugacheva, E., and Topalova, P. (2020), *The Effects of Weather Shocks on Economic Activity: What Are the Channels of Impact?*, «Journal of Macroeconomics», 65, 103207

Alessi, L., Barigozzi, M., and Capasso, M. (2010), *Improved Penalization for Determining the Number of Factors in Approximate Factor Models*, «Statistics and Probability Letters», 80, 23-24, pp. 1806-1813

Angeletos, G.-M., Collard, F., and Dellas, H. (2020), *Business-Cycle Anatomy*, «American Economic Review», 110, 10, pp. 3030-3070

Annicchiarico, B., Carattini, S., Fischer, C., and Heutel, G. (2021), *Business Cycles and Environmental Policy: Literature Review and Policy Implications*, Cambridge (MA), National Bureau of Economic Research

Auclert, A., Rognlie, M., and Straub, L. (2020), *Micro Jumps, Macro Humps: Monetary Policy and Business Cycles in an Estimated Bank Model*, National Bureau of Economic Research.

Barreca, A., Clay, K., Deschênes, O., Greenstone, M., and Shapiro, J.S. (2015), *Convergence in Adaptation to Climate Change: Evidence from High Temperatures and Mortality, 1900-2004*, «American Economic Review», 105, 5, pp. 247-251

Barsky, R. B., and Sims, E. R. (2011). *News Shocks and Business Cycles*, «Journal of Monetary Economics», 58, 3, pp. 273-289

Bastien-Olvera, B. A., Granella, F., and Moore, F.C. (2022), *Persistent Effect of Temperature on GDP Identified from Lower Frequency Temperature Variability*, «Environmental Research Letters», 17, 8

Bennedsen, M., Hillebrand, E., and Koopman, S.J. (2021), *Modeling, Forecasting, and Nowcasting US CO_2 Emissions Using Many Macroeconomic Predictors*, «Energy Economics», 96, 105118

Ben Zeev, N., and Khan, H. (2015), *Investment-Specific News Shocks and US Business Cycles*, «Journal of Money, Credit and Banking», 47, 7, pp. 1443-1464

Berg, K.A., Curtis, C.C., and Mark, N. (2023), *GDP And Temperature: Evidence On Cross-Country Response Heterogeneity*, National Bureau of Economic Research

Bernanke, B.S., Boivin, J., and Eliasz, P. (2005), *Measuring the Effects of Monetary Policy: A Factor-Augmented Vector Autoregressive (FAVAR) Approach*, «The Quarterly Journal of Economics», 120, 1, pp. 387-422

Bilal, A., and Känzig, D.R. (2024), *The Macroeconomic Impact of Climate Change: Global vs. Local Temperature*, National Bureau of Economic Research Working Paper Series

Burke, M., Hsiang, S.M., and Miguel, E. (2015, *Global Non-Linear Effect of Temperature on Economic Production*, «Nature», 527, 7577, pp. 235-239

Cai, Y., and Lontzek, T.S. (2019), *The Social Cost of Carbon With Economic and Climate Risks*, «Journal of Political Economy», 127, 6, pp. 2684-2734

Carleton, T., Jina, A., Delgado, M., Greenstone, M., Houser, T., Hsiang, S., *et al.* (2022), *Valuing the Global Mortality Consequences of Climate Change Accounting for Adaptation Costs and Benefits*, «The Quarterly Journal of Economics», 137, 4, pp. 2037-2105

Colacito, R., Hoffmann, B., and Phan, T. (2019), *Temperature and Growth: A Panel Analysis of The United States*, «Journal of Money, Credit and Banking», 51, 2-3, pp. 313-368

Conley, A., Westervelt, D., Lamarque, J.-F., Fiore, A., Shindell, D., Correa, G., and Horowitz, L. (2018), *Multimodel Surface Temperature Responses to Removal of US Sulfur Dioxide Emissions*, «Journal of Geophysical Research: Atmospheres», 123, 5, pp. 2773-2796

de Juan, A., Poncela, P., Rodríguez-Caballero, V., and Ruiz, E. (2022), *Economic Activity and Climate Change*, arXiv preprint arXiv, 2206.03187, https://arxiv.org/abs/2206.03187

Dell, M., Jones, B.F., and Olken, B.A. (2012), *Temperature Shocks And Economic Growth: Evidence From The Last Half Century*, «American Economic Journal: Macroeconomics», 4, 3, pp. 66-95

Deryugina, T., and Hsiang, S.M. (2014), *Does the environment still matter? Daily temperature and income in the United States*, National Bureau of Economic Research

Deschênes, O., and Greenstone, M. (2007), *The Economic Impacts of Climate Change: Evidence from Agricultural Output and Random Fluctuations in Weather*, «American Economic Review», 97, 1, pp. 354-385

DiCecio, R., and Owyang, M. (2010), *Identifying Technology Shocks in the Frequency Domain*, Federal Reserve Bank of St. Louis Working Paper No. 2010-060A

Dieppe, A., Francis, N., and Kindberg-Hanlon, G. (2021), *The Identification of Dominant Macroeconomic Drivers: Coping With Confounding Shocks*, ECB Working Paper No. 2021/2534

Donadelli, M., Jüppner, M., Riedel, M., and Schlag, C. (2017), *Temperature Shocks and Welfare Costs*, «Journal of Economic Dynamics and Control», 82, pp. 331-355

Erichson, N.B., Zheng, P., Manohar, K., Brunton, S.L., Kutz, J.N., and Aravkin, A.Y. (2020), *Sparse Principal Component Analysis Via Variable Projection*, «SIAM Journal on Applied Mathematics», 80, 2, pp. 977-1002

Fernald, J. (2014), *A Quarterly, Utilization-Adjusted Series on Total Factor Productivity*. Federal Reserve Bank of San Francisco Working Paper No. 2012-19

Forni, M., Gambetti, L., Antonio, G., Sala, L., and Soccorsi, S. (2023), *An American macroeconomic picture*, Mimeo, https://www.ssrn.com/abstract=3910770

Forni, M., Gambetti, L., and Sala, L. (2014), *No News in Business Cycles*, «The Economic Journal», 124, 581, pp. 1168-1191

Forni, M., Giannone, D., Lippi, M., and Reichlin, L. (2009), *Opening the Black Box: Structural Factor Models With Large Cross Sections*, «Econometric Theory», 25, 5, pp. 1319-1347

Foroni, C., Furlanetto, F., and Lepetit, A. (2018). *Labor supply factors and economic fluctuations*, «International Economic Review», 59, 3, pp. 1491-1510

Forster, P.M., Forster, H.I., Evans, M.J., Gidden, M.J., Jones, C.D., Keller, C.A., et al. (2020), *Current and Future Global Climate Impacts Resulting from COVID-19*, «Nature Climate Change», 10, 10, pp. 913-919

Fosten, J. (2019), *CO_2 Emissions and Economic Activity: A Short-To-Medium Run Perspective*, «Energy Economics», 83, pp. 415-429

Francis, N., and Ramey, V.A. (2009), *Measures Of Per Capita Hours And Their Implications For The Technology-Hours Debate*, «Journal of Money, Credit and Banking», 41, 6, pp. 1071-1097

Gali, J. (1999), *Technology, Employment, and the Business Cycle: Do Technology Shocks Explain Aggregate Fluctuations?*, «American Economic Review», 89, 1, pp. 249-271

Goulet Coulombe, P., and Göbel, M. (2021), *On Spurious Causality, CO_2, And Global Temperature*, «Econometrics», 9, 33

Gourio, F., and Fries, C. (2020), *Adaptation and the Cost of Rising Temperature for the US Economy*, *Mimeo*, //www.ssrn.com/abstract=3696920

Greene, C.A., Thirumalai, K., Kearney, K.A., Delgado, J.M., Schwanghart, W., Wolfenbarger, N.S., and Blankenship, D.D. (2019), *The Climate Data Toolbox for MATLAB*, Geochemistry, Geophysics, Geosystems

Hannachi, A., Jolliffe, I.T., and Stephenson, D.B. (2007), *Empirical Orthogonal Functions and Related Techniques in Atmospheric Science: A Review*, «International Journal of Climatology», 27, 9, pp. 1119-1152

Hsiang, S., Kopp, R., Jina, A., Rising, J., Delgado, M., Mohan, S., *et al.* (2017), *Estimating Economic Damage from Climate Change in the United States*, Science, 356, 6345, pp. 1362-1369

IPCC (2023), *AR6 Synthesis Report: Climate Change 2023*. Intergovernmental Panel on Climate Change, https://www.ipcc.ch/report/sixth-assessment-report-cycle/

Jones, M.W., Peters, G.P., Gasser, T., Andrew, R.M., Schwingshackl, C., Gütschow, J., and Le Quéré, C. (2023), *National Contributions to Climate Change Due to Historical Emissions of Carbon Dioxide, Methane, and Nitrous Oxide Since 1850*, «Scientific Data», 10, 1, p. 155

Joos, F., Roth, R., Fuglestvedt, J.S., Peters, G.P., Enting, I.G., Von Bloh, W., *et al.* (2013), *Carbon Dioxide and Climate Impulse Response Functions for the Computation of Greenhouse Gas Metrics: A Multi-Model Analysis*, «Atmospheric Chemistry and Physics», 13, 5, pp. 2793-2825

Jordà, Ò. (2005), *Estimation and Inference of Impulse Responses by Local Projections*, «American Economic Review», 95, 1, pp. 161-182

Justiniano, A., Primiceri, G.E., and Tambalotti, A. (2010), *Investment Shocks and Business Cycles*, «Journal of Monetary Economics», 57, 2, pp. 132-145

Justiniano, A., Primiceri, G.E., and Tambalotti, A. (2011), *Investment Shocks and the Relative Price of Investment*, «Review of Economic Dynamics», 14, 1, pp. 102-121

Kahn, M.E., Mohaddes, K., Ng, R.N., Pesaran, M.H., Raissi, M., and Yang, J.-C. (2021), *Long-Term Macroeconomic Effects of Climate Change: A Cross-Country Analysis*, «Energy Economics», 104, 105624

Kaufmann, R.K., Kauppi, H., Mann, M.L., and Stock, J.H. (2013), *Does Temperature Contain A Stochastic Trend: Linking Statistical Results to Physical Mechanisms*, «Climatic Change», 118, pp. 729-743

Khan, H., Metaxoglou, K., Knittel, C.R., and Papineau, M. (2019), *Carbon Emissions and Business Cycles*, «Journal of Macroeconomics», 60, pp. 1-19

Kilian, L. (1998), *Small-Sample Confidence Intervals for Impulse Response Functions*, «Review of Economics and Statistics», 80, 2, pp. 218-230

Kunkel, K.E., Stevens, L.E., Stevens, S.E., Sun, L., Janssen, E., Wuebbles, D., *et al.* (2013), *Regional Climate Trends and Scenarios for the US National Climate Assessment: Part 2. Climate Of The Southeast US*, NOAA Technical Report, https://www.ncdc.noaa.gov/assessment-report

Magnus, J.R., Melenberg, B., and Muris, C. (2011), *Global Warming and Local Dimming: The Statistical Evidence*, «Journal of the American Statistical Association», 106, 494, pp. 452-464

Mar, K.A., Unger, C., Walderdorff, L., and Butler, T. (2022), *Beyond CO_2 Equivalence: The Impacts of Methane on Climate, Ecosystems, and Health*, «Environmental Science and Policy», 134, pp. 127-136

Matsuura, K., and Willmott, C.J. (2018), *Terrestrial Air Temperature: 1900-2017 Gridded Monthly Time Series*, University of Delaware, Newark, http://climate.geog.udel.edu/~climate/html_pages/download.html#T2017

Montamat, G., and Stock, J.H. (2020), *Quasi-Experimental Estimates of The Transient Climate Response Using Observational Data*, «Climatic Change», 160, 3, pp. 361-371

Mumtaz, H., and Marotta, F. (2023), *Vulnerability to Climate Change: Evidence from a Dynamic Factor Model*, Mimeo, https://www.ssrn.com/abstract=3845743

Nath, I.B., Ramey, V.A., and Klenow, P.J. (2023), *How Much Will Global Warming Cool Global Growth?*, Working Paper, https://doi.org/10.2139/ssrn.4358324

Natoli, F. (2023), *The Macroeconomic Effects of Temperature Surprise Shocks*, SSRN 4160944. https://doi.org/10.2139/ssrn.4160944

Newell, R.G., Prest, B.C., and Sexton, S.E. (2021), *The GDP-Temperature Relationship: Implications for Climate Change Damages*, «Journal of Environmental Economics and Management», 108, 102445

NOAA (2023), *What are La Niña and El Niño and why do they matter?*, ENSO Fact Sheet, https://www.noaa.gov/enso

Peersman, G., and Straub, R. (2009), *Technology Shocks and Robust Sign Restrictions in a Euro Area SVAR*, «International Economic Review», 50, 3, pp. 727-750

Phillips, P.C., Leirvik, T., and Storelvmo, T. (2020), *Econometric Estimates of Earth's Transient Climate Sensitivity*, «Journal of Econometrics», 214, 1, pp. 6-32

Pretis, F. (2020), *Econometric Modelling of Climate Systems: The Equivalence of Energy Balance Models and Cointegrated Vector Autoregressions*, «Journal of Econometrics», 214, 1, pp. 256-273

Pretis, F. (2021), *Exogeneity in Climate Econometrics*, «Energy Economics», 96, 105122

Ramey, V.A. (2016), *Macroeconomic shocks and their propagation*, in J.B. Taylor and H. Uhlig (eds), *Handbook of Macroeconomics*, Elsevier, vol. 2, pp. 71-162

Ricke, K.L., and Caldeira, K. (2014), *Maximum Warming Occurs About One Decade After a Carbon Dioxide Emission*, «Environmental Research Letters», 9, 12, 124002

Shapiro, M.D., and Watson, M.W. (1988), *Sources of Business Cycle Fluctuations*, in S. Fisher and C.S. Black (eds), *NBER Macroeconomics Annual*, Cambridge (MA),The Mit Press, vol. 3, pp. 111-148

Smith, S.J., van Aardenne, J., Klimont, Z., Andres, R.J., Volke, A., and Delgado Arias, S. (2011), *Anthropogenic Sulfur Dioxide Emissions: 1850-2005*, «Atmospheric Chemistry and Physics», 11, 3, pp. 1101-1116

Stock, J.H. (2020), *Climate change, climate policy, and economic growth*, in J.B. Taylor and H. Uhlig (eds), *NBER Macroeconomics Annual*, Cambridge (MA), The Mit Press, vol. 34, pp. 399-419). MIT Press.

Storelvmo, T., Leirvik, T., Lohmann, U., Phillips, P.C., and Wild, M. (2016), *Disentangling Greenhouse Warming and Aerosol Cooling to Reveal Earth's Climate Sensitivity*, «Nature Geoscience», 9, 4, pp. 286-289

Uhlig, H. (2003), *What Drives GNP?*, Unpublished manuscript, Euro Area Business Cycle Network, https://www.euro-area-bcn.org/papers/uhlig_gnp.pdf

Wieland, V., Afanasyeva, E., Kuete, M., and Yoo, J. (2016), *New Methods For Macro-Financial Model Comparison and Policy Analysis*, in J.B. Taylor and H. Uhlig (eds), *Handbook of Macroeconomics*, Elsevier, vol. 2, pp. 1241-1319

Wieland, V., Cwik, T., Müller, G.J., Schmidt, S., and Wolters, M. (2012), *A New Comparative Approach to Macroeconomic Modeling and Policy Analysis*, «Journal of Economic Behavior and Organization», 83, 3 pp. 523-541

Zickfeld, K., and Herrington, T. (2015), *The Time Lag Between a Carbon Dioxide Emission and Maximum Warming Increases With the Size of the Emission*, «Environmental Research Letters», 10, 3, 031001

APPENDIX

A DATA CONSTRUCTION

We follow Angeletos et al. (2020) in constructing the economic variables.

TABLE 5 • ECONOMIC DATA SOURCES AND TRANSFORMATIONS

Data	FRED Mnemonic	Frequency/Transformation
Real gross domestic product per capita	A939RX0Q048SBEA	Q
Real Gross domestic product	GDPC1	Q
Share of GDP: gross private domestic investment	A006RE1Q156NBEA	Q
Share of GDP: personal consumption expenditures: durable goods	DDURRE1Q156NBEA	Q
Nonfarm business sector: average weekly hours	PRS85006023	Q
Employment Level	CE16OV	M2Q (EoP)
Total factor productivity (annualized Q-Q growth rate)	dTFPu (from Fernald)	Q

The variables enter the model as follows:

1. **Real GDP**: log(GDPC1) × 100
2. **Real investment**: log((DDURRE1Q156NBEA + A006RE1Q156NBEA) × GDPC1) × 100
3. **Hours**: log(PRS85006023 × CE16OV) × 100
4. **TFP**: cumsum(dTFPU/400) × 100
5. **Population**: GDPC1/A939RX0Q048SBEA

For checks, the variables real GDP, real investment, and hours can be transformed to per capita units by dividing by the population level as computed above before taking logs.

B BOOTSTRAP PROCEDURE

We compute confidence bands for the IRFs and the cyclical variances using the following bootstrap procedure:

1. 1.Use (2) to generate a new vector $\boldsymbol{Y_t}$by bootstrapping from the reduced form residuals.
2. Use the method of Kilian (1998) to correct the bias of the OLS estimates.
3. Use $\boldsymbol{\Lambda}$ to recompute the common component of temperatures, $\boldsymbol{\Lambda Y_t}$, and add the original idiosyncratic component, $\boldsymbol{\eta}_{it}$, to get a new data set of US temperatures.
4. On this new data set, estimate r = 8 principal components, and re-estimate a bootstrap $\boldsymbol{\Lambda_B}$.
5. Estimate the FAVAR in (2) again with $\boldsymbol{p = 2}$.

6. Identify the shocks sequentially, compute IRFs and the cyclical variances.
7. Repeat this 1, 500 times to obtain bootstrap distributions of the IRFs and the cyclical variances.
8. Find the quantiles of the bootstrap distributions to get the 68% and 90% intervals.

C ROBUSTNESS CHECKS

To test the sensitivity of our results to the underlying assumptions, we conduct the following robustness checks:

1. Changing the number of temperature factors:
We originally used a statistical criterion to determine the number of factors to be extracted from the gridded temperature dataset, opting for r=8 for parsimony. The upper bound recommended by the criterion was r=17, which we also test. In this case, we set p=1 according to the Bayesian Information Criterion (BIC).

2. More lags:
Our results focus primarily on the low-frequency components of temperatures. To address potential inaccuracies due to a very short lag length, we test an increased lag length. In the baseline specification, p=2; here, we increase this to p=4. Given the frequentist approach to estimation, results become quite erroneous for even larger lag orders.

3. Sub-sample analysis (1970):
The dataset used spans from 1948 to 2017. The trend in temperatures attributed to human influence becomes very pronounced around 1970. Additionally, SO_2 emissions in the US start to decline from the 1970s. We repeat our analysis by excluding the first 22 years from the sample to observe any changes.

4. Potential interference from outside shocks:
Non-US shocks may drive business cycle (BC) and low-frequency (LF) variation in US aggregates, affecting temperatures. Although the US is typically considered to have frontier technology (Nath *et al.*, 2023), shocks from China might spill over and be misidentified as US shocks. Given the challenge of obtaining long quarterly time series for China, we use annual series for CO_2 emissions, which show a significant increase from 2000. We thus cut the sample at Q4:1999 to check for potential external influences from China.

5. Maximizing long-run IRFs instead of variances:
As an alternative to maximizing variances, we explore maximizing the long-run IRF of Total Factor Productivity (TFP) and hours, as suggested in Forni *et al.* (2014). This approach is crucial since the connection between the economy and temperatures largely runs through TFP, making accurate identification of the technology shock essential.

6. Variables in per capita terms:

Long-run economic dynamics may be affected by demographic changes (Francis and Ramey, 2009), which are not explicitly accounted for in our baseline specification. Population changes are a significant source of emission variations according to the Kaya identity. We check whether expressing economic variables (GDP, hours, and investment) in per capita terms alters our results.

Robustness Results:

The results are generally insensitive to changes in lag order, number of factors, or specification of variables in per capita terms. Minor changes are observed for sub-samples and when altering the long-run identification assumption, as detailed in robustness check 5. Figure 12 illustrates the IRFs for average US temperatures in response to economic shocks. The most notable differences occur when changing the sub-samples to post-1970 and pre-2000. In these cases, the technology shock leads to positive temperature responses due to the diminished role of SO_2 emissions and other aerosols in cooling temperatures after 1970. Similarly, excluding the more recent period attributes some cooling to the investment shock, as the reduction in SO_2 emissions has not yet fully materialized. These changes, while interesting, underscore the significance of this additional channel for the transmission of economic activity to temperature changes.

FIGURE 12 • IMPULSE RESPONSE FUNCTIONS OF US AVERAGE TEMPERATURES TO ECONOMIC SHOCKS FOR ROBUSTNESS CHECKS 1-6.

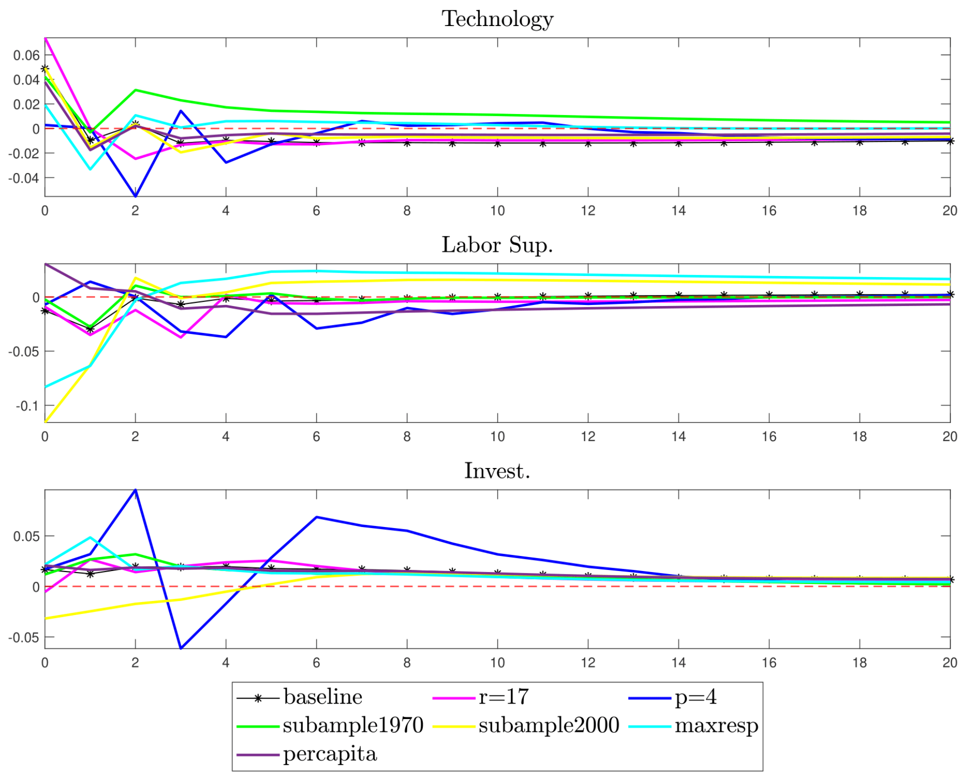

Figure 13, on the other hand, reports the IRFs of real GDP to the different temperature shocks for all robustness checks. We observe that changing the number of temperature principal components or the number of lags has negligible effects on the IRFs compared to our baseline specification. The same goes for taking the variables in per capita terms. Changes in the responses of GDP to the temperature shocks are slightly more pronounced if we use labor productivity instead of TFP or the maximal response identification strategy to obtain the technology shock and then condition the temperature shocks on it. All in all, the baseline specification lies roughly in the middle of the IRFs under the different robustness checks. We leave the robustness check IRFs of the economic variables to the economic shocks in the Appendix since the only minor difference arises when using the response maximization approach over the cyclical variance maximization approach.

FIGURE 13 • IMPULSE RESPONSE FUNCTIONS OF GDP TO TEMPERATURE SHOCKS FOR ROBUSTNESS CHECKS 1-6

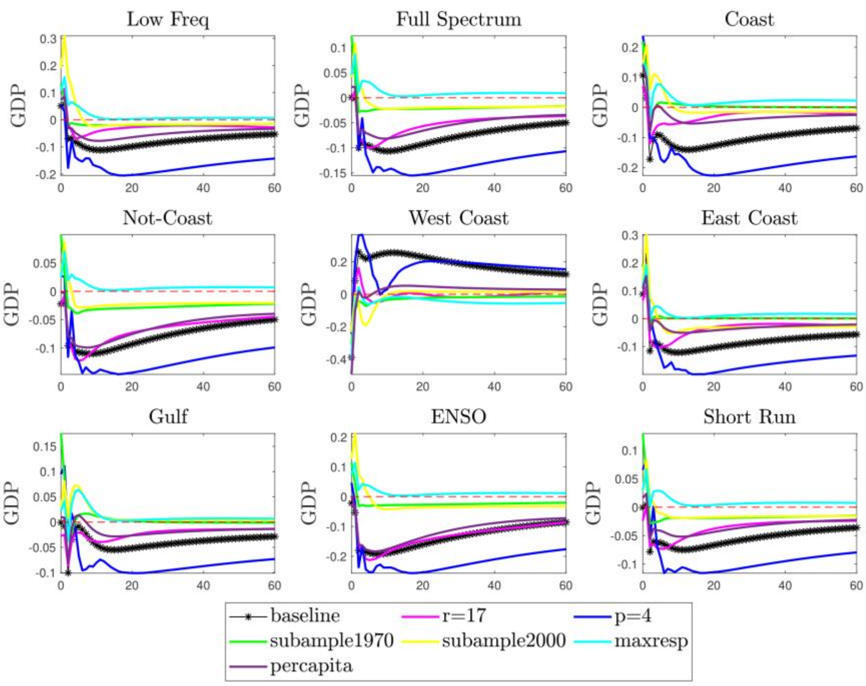

FIGURE 14 • IMPULSE RESPONSE FUNCTIONS OF ECONOMIC VARIABLES TO ECONOMIC SHOCKS FOR ROBUSTNESS CHECKS 1-6.

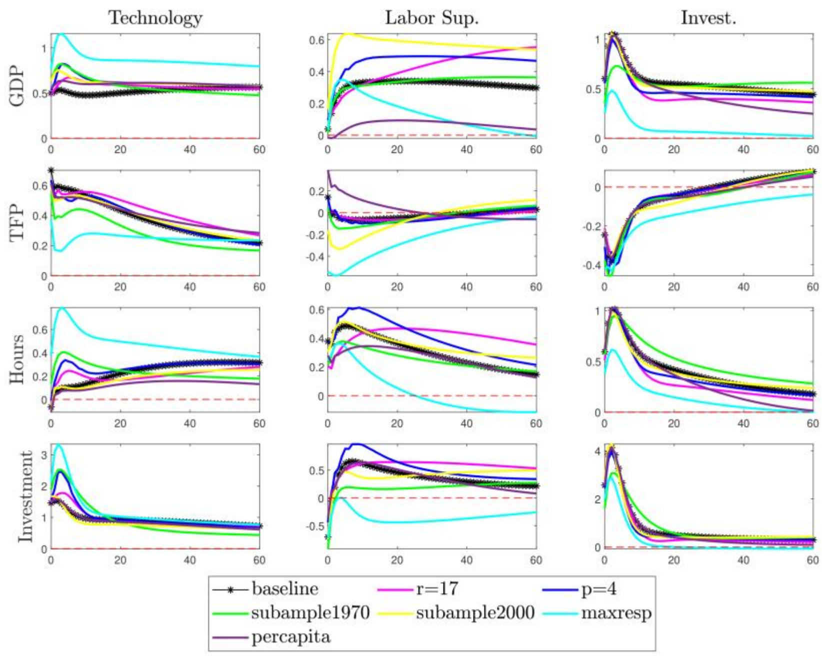

Lastly, we check if the sequence of conditional identifications matters for our results. We therefore permute the identification order of the three economic shocks – technology (T), investment (I) and labor supply (H) – to allow for all possible orderings and report the economic and temperature IRFs.

FIGURE 15 • IMPULSE RESPONSE FUNCTIONS OF ECONOMIC VARIABLES FOR DIFFERENT ORDERINGS OF IDENTIFICATION.

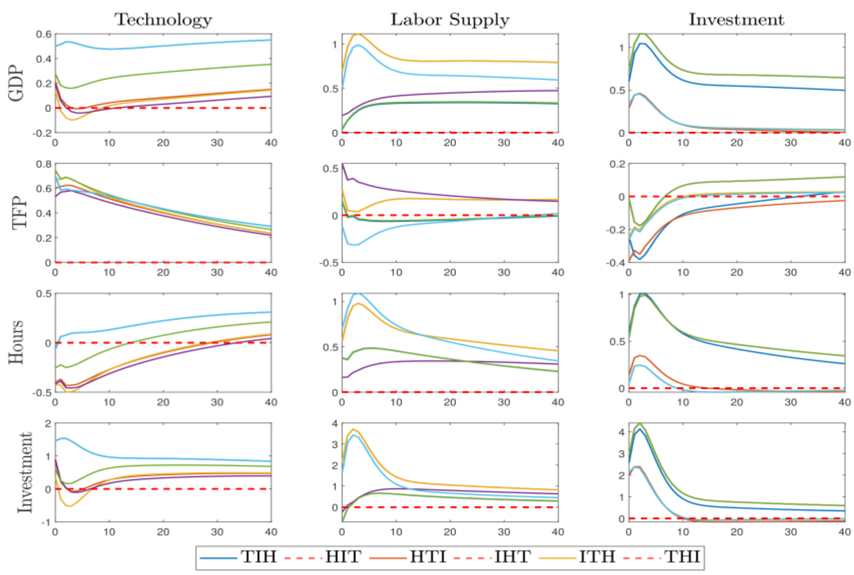

FIGURE 16 • IMPULSE RESPONSE FUNCTIONS OF AVERAGE TEMPERATURES FOR DIFFERENT ORDERINGS OF IDENTIFICATION

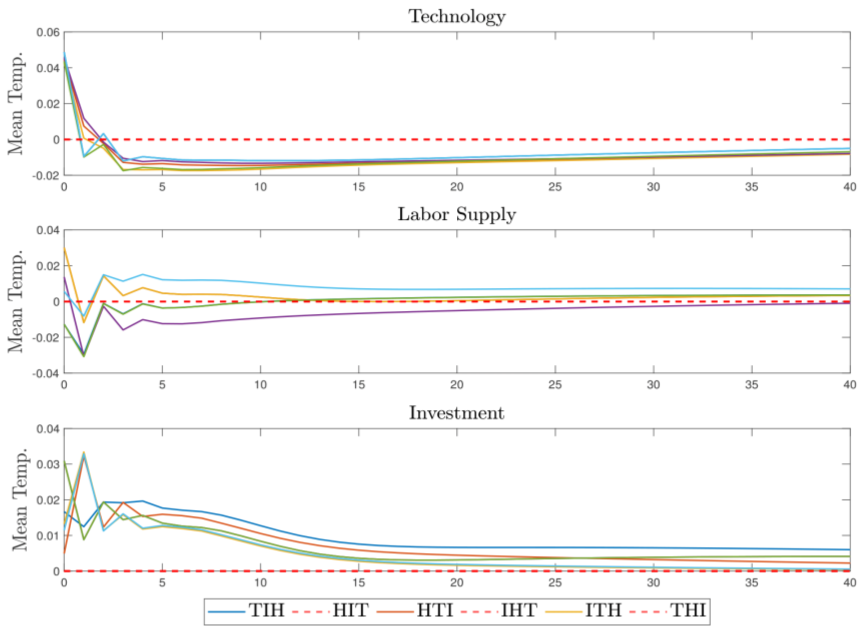

Figures 15 and 16 show that while there are some differences in the responses of the economic variables if the investment shock is identified first, these do not translate to changes in the more important results for temperature changes following the economic expansions.

D Simulation Exercise

We simulate 1,000 instances of the model proposed by Justiniano *et al.* (2011) using the Macroeconomic Model Data Base in Dynare (Wieland *et al.*, 2012, 2016), adhering to the standard settings without modifications. Each simulation includes data for GDP, Total Factor Productivity (TFP), hours worked, and investment, along with additional series that are not considered for this exercise. For each of the 1,000 simulations, we extract the true Impulse Response Functions (IRFs) for neutral technology shocks, investment shocks, and wage markup shocks (which have a similar interpretation to our labor supply shocks). We then apply our sequential identification strategy to identify these three structural shocks in the frequency domain using a VAR(4) model with the four economic time series of interest.

In the model of Justiniano *et al.* (2011), the neutral technology shock is the sole driver of TFP growth, the wage markup shock is the primary factor influencing low-frequency changes in hours worked, and the investment shock predominantly affects investment variation in the business cycle band. Consequently, our identification approach is theoretically validated for this case.

FIGURE 17 • IMPULSE RESPONSE FUNCTIONS OF ECONOMIC VARIABLES TO ECONOMIC SHOCKS FROM SIMULATED DATA AS PER JUSTINIANO *ET AL.* (2011)

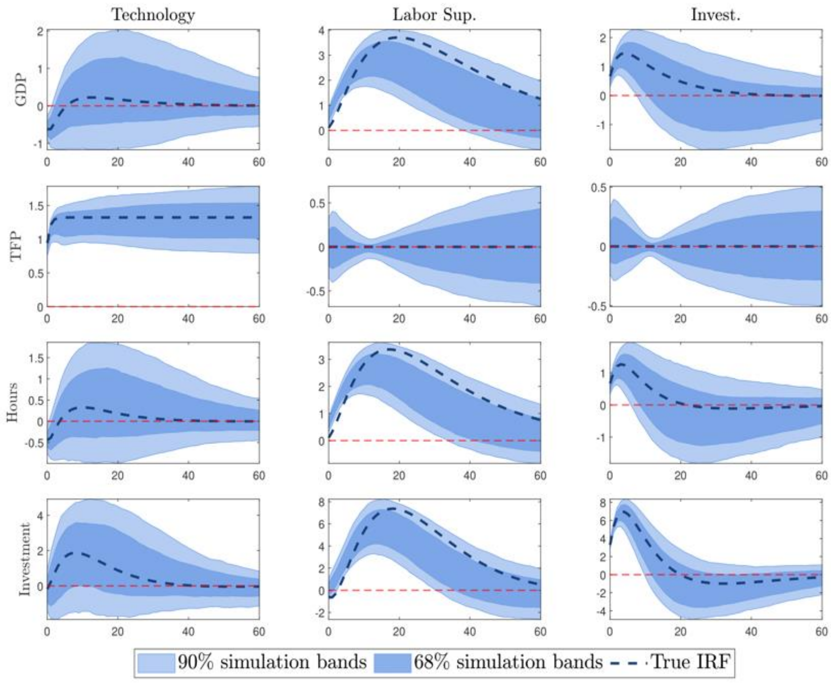

Figure 17 shows the bands resulting from the 1,000 identification exercises on simulated data as well as the theoretically true IRFs. Our VAR-based approach is very successful in capturing the correct dynamics in the vast majority of the simulation runs. This gives us confidence that it may also be useful in a purely applied setting.